

Synthesis, Structure, and Reactivity of Uranium(VI) Nitrides

Luciano Barluzzi, Fang-Che Hsueh, Rosario Scopelliti, Benjamin Atkinson, Nikolas Kaltsoyannis, and Marinella Mazzanti*

Institut des Sciences et Ingénierie Chimiques, Ecole Polytechnique Fédérale de Lausanne (EPFL), 1015 Lausanne, Switzerland

Department of Chemistry, University of Manchester, Oxford Road, Manchester, M13 9PL, UK

Electronic Supplementary Information (ESI)

Table of Contents

Materials and Methods	2
NMR Spectra	12
X-ray Crystallographic Details and Refinement Data	31
IR Spectra	36
GC-MS experiment	38
Computational Details	39
References	41

Materials and Methods

General Considerations. The syntheses and manipulations described below were conducted under argon or nitrogen with rigorous exclusion of air and water using an MBraun glovebox equipped with a purifier unit that kept oxygen and water level below 0.1 ppm along with vacuum and Schlenk line techniques. Glassware was dried at 150°C before use. Anhydrous solvents were purchased from Aldrich and further distilled from K/benzophenone (THF, toluene). Depleted uranium turnings were purchased from IBILABS, Florida (USA). Deuterated solvents for NMR spectroscopy (d_8 -thf, d_8 -toluene) were purchased from Cortecnet, freeze-degassed and distilled over K/benzophenone. d_6 -dmso was freeze-degassed and dried over 3 Å molecular sieves for several days. Unless otherwise noted, reagents were purchased from commercial suppliers and used as received. $[K_2\{U(OSi(O^tBu)_3)_3(\mu-N)\}_2]$, **1**,¹ $[K_2\{U(OSi(O^tBu)_3)_3(\mu-NH)\}_2]$, **6**,¹ NEt_3HBPh_4 ,² and $AgBPh_4$ ³ were prepared as previously described. CO (N47 Bt-S 10/200) was purchased from Carbagas and stored over activated 3 Å molecular sieves. H₂ (99.9999% purity) was purchased from Carbagas. ¹³CO (93.13% ¹³C) and D₂ (99.8% D) were purchased from Cortecnet and transferred to a flask containing activated 3 Å molecular sieves prior to use. Elemental analyses were performed under nitrogen with a ThermoScientific Flash 2000 Organic Elemental Analyzer. NMR experiments were carried out using NMR tubes adapted with J. Young valves. ¹H and ¹³C spectra were recorded using Avance 400 MHz (¹³C 125 MHz) or Avance III-HD 600 MHz (¹³C 151 MHz) NMR spectrometers and chemical shifts were referenced internally to residual proteo-solvent references.

Caution: *Depleted uranium (primary isotope ²³⁸U) is a weak α -emitter (4.197 MeV) with a half-life of 4.47×10^9 years. Manipulations and reactions should be carried out in monitored fume hoods or in an inert glovebox in a radiation laboratory equipped with α - and β -counting equipment.*

GC-MS experiments.

GC-MS analysis of headspace from the decomposition reaction of isolated complex **4** was performed under Ar using a Thermo Fisher Trace 1300 GC equipped with a TGBond Msieve 5A column (30m x 0.32 mm x 30 μ m) coupled to Thermo Fisher TSQ8000 MS. The reaction was conducted in a J-Young adapted NMR tube. The headspace was recovered with a syringe from a septum and immediately injected into the instrument. Control experiment were carried out by injecting headspace from solutions of complex **2** (which does not release N₂).

Synthetic procedures.

Synthesis of [K{U(OSi(O^tBu)₃)₃(μ -N)}₂], **2.** In a nitrogen-filled glovebox, a solution of [K₂{U(OSi(O^tBu)₃)₃(μ -N)}₂], **1** (65.7 mg, 0.03 mmol, 1 equiv) in 3 mL of toluene was poured onto solid AgBPh₄ (26.0 mg, 0.06 mmol, 2 equiv). The solution was stirred overnight at room temperature. Thereafter, the reaction mixture changed colour from dark brown to orange-brown and a dark precipitate formed. The reaction mixture was centrifuged to remove solid Ag⁰ and KBPh₄. The supernatant was then evaporated (1 mL) and left standing at -40°C overnight affording brown-orange crystals of [K{U(OSi(O^tBu)₃)₃(μ -N)}₂], **2** (39.5 mg, yield=62%). ¹H NMR (400 MHz, *d*₈-toluene, 298 K): δ 0.6 ppm (br s, -OSi(O^tBu)₃, 162H). Anal. Calcd for CHN₂O₂₄Si₆U₂: C, 40.72; H, 7.69; N, 1.32. Found: C, 40.33; H, 7.21; N, 1.33.

When the reaction was performed with 1 equiv of AgBPh₄, the slower consumption of the starting material (5 days) was observed but resulted in the formation of the same final reaction mixture as evidenced by ¹H NMR spectroscopy (Figure S1).

Synthesis of $[\text{K}_2\{\text{U}(\text{OSi}(\text{O}^t\text{Bu})_3)_3\}_2(\mu\text{-N})_2(\mu\text{-I})]$, **3.** In an argon-filled glovebox, solid I_2 (1.3 mg, 0.005 mmol, 0.5 equiv) was added to a solution of $[\text{K}_2\{\text{U}(\text{OSi}(\text{O}^t\text{Bu})_3)_3(\mu\text{-N})\}_2]$, **1** (21.9 mg, 0.01 mmol, 1 equiv) in 0.5 mL of d_8 -toluene. The reaction mixture immediately changed colour from dark brown to orange. The ^1H NMR spectrum of the reaction mixture (Figure S4) revealed the immediate consumption of the starting material. The reaction mixture was filtered on a 0.2 μm porosity filter frit and the filtrate was left standing at -30°C overnight affording ochre yellow crystals of $[\text{K}_2\{\text{U}(\text{OSi}(\text{O}^t\text{Bu})_3)_3\}_2(\mu\text{-N})_2(\mu\text{-I})]$, **3** (13.8 mg, yield=60%). ^1H NMR (400 MHz, d_8 -toluene, 298 K): δ 0.7 ppm (br s, $-\text{OSi}(\text{O}^t\text{Bu})_3$, 162H). Anal. Calcd for $\text{CHN}_2\text{O}_{24}\text{Si}_6\text{U}_2(\text{C}_7\text{H}_8)_{0.7}$: C, 39.23; H, 7.18; N, 1.19. Found: C, 39.16; H, 7.55; N, 1.13.

Reaction of complex $[\text{K}_2\{\text{U}(\text{OSi}(\text{O}^t\text{Bu})_3)_3(\mu\text{-N})\}_2]$, **1 with 10 equiv of AgBPh_4 .** In a nitrogen-filled glovebox, a solution of $[\text{K}_2\{\text{U}(\text{OSi}(\text{O}^t\text{Bu})_3)_3(\mu\text{-N})\}_2]$, **1** (17.6 mg, 0.008 mmol, 1 equiv) in 0.5 mL of d_8 -toluene was added to solid AgBPh_4 (34.8 mg, 0.08 mmol, 10 equiv). The reaction mixture was analyzed by ^1H NMR spectroscopy and the only observable species was $[\text{U}(\text{OSi}(\text{O}^t\text{Bu})_3)_4]$ (Figure S6).

Reaction of complex $[\text{K}_2\{\text{U}(\text{OSi}(\text{O}^t\text{Bu})_3)_3(\mu\text{-N})\}_2]$, **1 with 2 equiv of I_2 .** In an argon-filled glovebox, solid I_2 (1.8 mg, 0.0072 mmol, 2 equiv) was added to a solution of $[\text{K}_2\{\text{U}(\text{OSi}(\text{O}^t\text{Bu})_3)_3(\mu\text{-N})\}_2]$, **1** (7.8 mg, 0.0036 mmol, 1 equiv) in 0.5 mL of d_8 -toluene. The reaction mixture changed colour from dark brown to red and a colourless precipitate of presumably KI was formed. The reaction mixture was analyzed by ^1H NMR spectroscopy after one night, revealing the formation of an intractable reaction mixture (Figure S7).

Synthesis of $[\{U(OSi(O^tBu)_3)_3\}_2(\mu-N)_2(\mu-thf)]$, **4.** In a nitrogen-filled glovebox, a blue suspension of $[N(C_6H_4Br)_3][SbCl_6]$ (45.3 mg, 0.0056 mmol, 2 equiv) in 0.5 mL of thf was added to a dark brown solution of $[K_2\{U(OSi(O^tBu)_3)_3(\mu-N)\}_2]$, **1** (60 mg, 0.028 mmol, 1 equiv) in 0.5 mL of thf. Over the course of few minutes, the blue ammonium salt was fully consumed and the colour of the reaction mixture changed from dark brown to red-orange. The reaction mixture was divided into two portions of 0.5 mL. The solvent was removed from each fraction independently while keeping them at -80°C . The resultant red-orange solid residues were both dissolved in a total of 0.4 mL of toluene. The resulting suspension was filtered on a $0.2\ \mu\text{m}$ porosity filter frit and the filtrate was left standing at -40°C overnight yielding red-orange crystals of complex $[\{U(OSi(O^tBu)_3)_3\}_2(\mu-N)_2(\mu-thf)]$, **4** (21.1mg, yield=35%). ^1H NMR (400 MHz, d_8 -thf, 298K): δ 1.44 ppm (s, $-OSi(O^tBu)_3$, 162H). ^1H NMR (400 MHz, d_8 -toluene, 298K): δ 1.69 ppm (s, $-OSi(O^tBu)_3$, 162H). Anal. Calcd for $C_{72}H_{162}O_{24}N_2Si_6U_2$: C, 41.63; H, 7.44; N, 1.19. Found: C, 41.48; H, 7.83; N, 1.34. Quantitative ^1H NMR spectroscopy by comparison with a $O(SiMe_3)_2$ internal standard revealed 94% conversion of **1** into **4**, but the high solubility of **4** together with the used synthetic method prevents the obtention of larger isolated yields. Solvent removal at -80°C is necessary due to the decomposition of complex **4** under vacuum at room temperature. When the solvent removal from the reaction mixture is performed at room temperature a mixture of light green-blue and red solids is formed. If the solid is maintained under dynamic vacuum for additional 15 minutes, only light green-blue solids can be observed. The ^1H NMR spectrum of the green residue does not show the presence of complex **4** but a mixture of unidentified species (Figure S11). When the reaction mixture is dried at -80°C over the course of 8h only the signals of complex **4** are observed (Figure S12). If more than 0.5 mL of the reaction

mixture are dried at -80°C, the longer times needed for the evaporation of the solvent leads to the formation of decomposition products (Figure S13).

Stability of complex 4 in the reaction mixture under argon. Complex 4 was formed *in situ* as described above. The evolution of the reaction mixture was monitored for 5 days by ¹H NMR spectroscopy at room temperature. The colour of the reaction mixture changed slowly over time to light green and complex 4 was fully consumed after 5 days yielding a complex mixture of species (Figures S14). Removal of volatiles from the reaction mixture and subsequent dissolution of the green-blue residue in toluene (0.5 mL) afforded a suspension that was filtered on a 0.2 µm filter frit. The resulting solution left standing at -40°C overnight yielded light blue crystals of the complex [U(OSi(O^tBu)₃)₃Cl(thf)₂], 5.

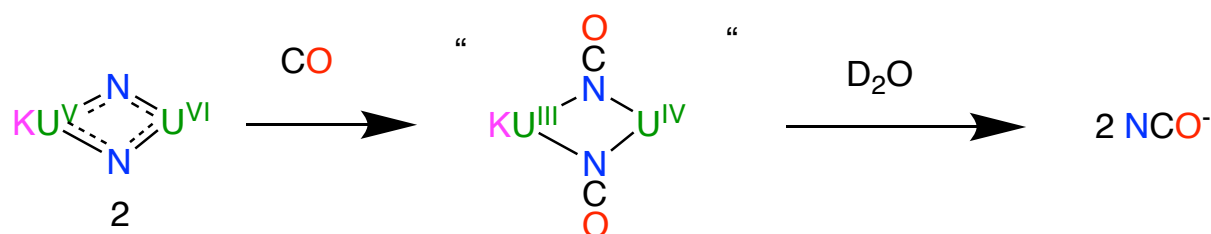
Stability of isolated complex 4 under Ar. In an argon-filled glovebox, complex 4 (9.1 mg, 0.0042 mmol) was dissolved in 0.5 mL of *d*₈-thf. The evolution of the composition of the solution was monitored by ¹H NMR spectroscopy, revealing the full consumption of complex 4 after 5 days and the formation of an intractable mixture of products (Figure S16).

After full decomposition of complex 4, the headspace of the reaction mixture was analyzed in a GC-MS spectrometer, revealing the formation of N₂ (Figure S45). Thereafter, volatiles were removed under vacuum and an excess (200 µL) of a 2M solution of HCl in Et₂O was added to the yellow solid residue. The reagents were left reacting for 15 minutes and volatiles were removed under vacuum affording a colourless precipitate. *d*₆-dmsO was added to the solid residue. A known amount of dimethylsulfone was added as an internal standard. ¹H NMR studies revealed the formation of only trace amounts (1.5%) of NH₄Cl (Figure S18).

Stability of isolated complex 4 under vacuum. In an argon-filled glovebox, complex **4** (8.3mg, 0.0038 mmol) was dissolved in 0.5 mL of d_8 -thf. Upon exposure of the solution to dynamic vacuum, light brown solids start to form while the red solution evaporates. Upon complete removal of the solvent light brown-yellow solids form. The solid residue was exposed to dynamic vacuum for additional 15 minutes and then it was dissolved in d_8 -thf yielding a yellow-light brown solution. Analysis of the reaction mixture by ^1H NMR spectroscopy revealed the full consumption of complex **4** and the formation of an intractable mixture of products (Figure S19) identical to that formed upon decomposition of isolated complex **4** under Ar.

Reaction of complex 2 with CO. In a nitrogen-filled glovebox, complex $[\text{K}\{\text{U}(\text{OSi}(\text{O}^t\text{Bu})_3)_3(\mu\text{-N})\}_2]$, **2** (10.4 mg, 0.0049 mmol, 1 equiv) was dissolved in 0.5 mL of d_8 -toluene and the solution was transferred into an NMR tube equipped with a J-Young valve. The NMR tube was connected to a Schlenck line and the solution was degassed by three cycles of freeze-pump-thawing. 1 atm of ^{13}C O was added to the tube. The reaction mixture changed colour from brown-orange to light green over the course of 30 minutes. ^1H NMR studies showed the formation of an intractable mixture of compounds (Figure S20). The ^{13}C NMR spectrum of the reaction mixture showed the presence of two peaks at 215.71 and at -162.60 ppm attributed to U-bound ^{13}C -containing species (Figure S21). Volatiles were removed and 0.5 mL of pD=12 D_2O were added to the resultant light green solid together with few drops of d_6 -dmsO as a reference. The ^{13}C NMR spectrum of the reaction mixture in D_2O showed the presence of N^{13}CO^- (Figure S22). Quantitative ^{13}C NMR spectroscopy, performed with $\text{CH}_3^{13}\text{COONa}$ as external standard, revealed the presence of 2 equiv of

N^{13}CO^- per complex. These results indicate that both nitrides undergo reductive carbonylation according to Scheme S1.



Scheme S1. Reaction of complex 2 with CO

Reactivity of complex 4 with CO and H₂. Upon addition of 1 atm of CO to a degassed thf or toluene solution of 4, the ¹H NMR spectrum (Figures S23-S24) showed no reaction between complex 4 and CO, but only the formation of decomposition products over the course of 5 days. Volatiles were removed and 0.5 mL of pD=12 D₂O were added to the resultant light green solid together with few drops of *d*₆-dmso as a reference. The ¹³C NMR spectrum of the reaction mixture quenched in D₂O did not show the presence of ¹³C-containing species. Similarly, after addition of 1 atm H₂ to a solution of to a degassed thf or toluene solution of 4 no reaction was observed.

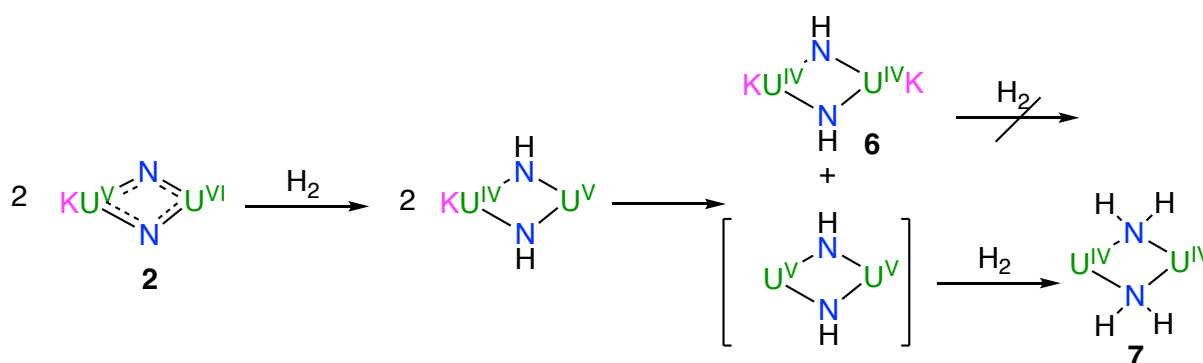
Reaction of complex 2 with H₂ and isolation of the complexes [K₂{U(OSi(O^tBu)₃)₃(μ-NH)}₂], 6 and [{U(OSi(O^tBu)₃)₃}₂(μ-NH₂)₂(μ-thf)], 7. In a nitrogen-filled glovebox, complex [K{U(OSi(O^tBu)₃)₃(μ-N)}₂], 2 (13.3 mg, 0.006 mmol, 1 equiv) was dissolved in 0.5 mL of *d*₈-toluene and the solution was transferred into an NMR tube equipped with a J-Young valve. The NMR tube was connected to a Schlenck line and the solution was degassed by three cycles of freeze-pump-thawing. 1 atm of H₂ was added to the tube. The reaction mixture

slowly changed colour from brown-orange to green over the course of 2 days. ^1H NMR studies revealed the slow conversion of complex **2** to an equimolar mixture of two species (Figure S25). No intermediate species could be observed. Volatiles were removed and the resulting residue was dissolved in 0.3 mL of Et_2O . One drop of thf was added to the reaction mixture and the solution was left standing at -40°C affording yellow crystals of the previously reported complex $[\text{K}_2\{\text{U}(\text{OSi}(\text{O}^t\text{Bu})_3)_3(\mu\text{-NH})_2\}]$, **6**¹ and light green crystals of complex $[\{\text{U}(\text{OSi}(\text{O}^t\text{Bu})_3)_3\}_2(\mu\text{-NH}_2)_2(\mu\text{-thf})]$, **7** that were characterized by XRD studies. The D-labelled mixture of D-**6** and D-**7** was prepared using the same procedure from D_2 .

The formation of complexes **6** and **7** is believed to proceed according to Scheme S2.

Due to the similar solubility the two complexes, complex **7** cannot be obtained analytically pure from this reaction.

In an experiment carried out with the same procedure, after the reaction was finished, the volatiles were removed and 300 μL of a 2M solution of HCl in Et_2O were added to the solid residue. After 10 minutes, volatiles were removed under vacuum. The resultant solid was dissolved in 0.5 mL of d_6 -dmsO and dimethylsulfone was added as an internal standard for the quantitative NH_4Cl detection. NH_4Cl is formed in 72% yield. (Figure S29)



Scheme S2. Proposed mechanism for the formation of the complexes **6** and **7** upon hydrogenation of complex **2**.

Independent synthesis of $[\{U(OSi(O^tBu)_3)_3\}_2(\mu-NH_2)_2]$, **7.** In a nitrogen-filled glovebox, a solution of NEt_3HBPh_4 (10.2 mg, 0.024 mmol, 2 equiv) in 0.5 mL of thf was added to a solution of complex $[K_2\{U(OSi(O^tBu)_3)_3(\mu-NH)\}_2]$, **6** (25.9 mg, 0.012 mmol, 1 equiv) in 0.5 mL of thf. The reaction mixture immediately changed colour from yellow to green and colourless precipitate of $KBPh_4$ formed. 1H NMR studies revealed the clean formation of a new species (Figure S30). Volatiles were removed and 0.5 mL of toluene were added to the resultant green solid residue. The reaction mixture was filtered and the resultant green solution was left standing at $-40^\circ C$ affording light green crystals of $[\{U(OSi(O^tBu)_3)_3\}_2(\mu-NH_2)_2]$, **7** (15.8 mg, yield= 62.4%) 1H NMR (400 MHz, d_8 -thf, 298 K): δ -0.21 (s, $-OSi(O^tBu)_3$, 162H) ppm, 1H NMR (400 MHz, d_8 -toluene, 298 K): δ -0.21 (s, $-OSi(O^tBu)_3$, 162H) ppm. Anal. Calcd for $C_{72}H_{166}N_2O_{24}Si_6U_2(C_7H_8)_{0.7}$: C, 42.90%; H, 8.03% ; N, 1.30%. Found: C, 42.88%; H, 8.37%; N, 1.66%. Crystals of $[\{U(OSi(O^tBu)_3)_3\}_2(\mu-NH_2)_2(\mu-thf)]$, **7** suitable for XRD studies were obtained by cooling down a concentrated solution of **7** in Et_2O at $-40^\circ C$.

Attempts to oxidize complex **6** using “magic blue” resulted in a mixture of multiple products including a chloride abstraction product (the mixed valent U(V)U(VI) diimido chloride $[\{U(OSi(O^tBu)_3)_3\}_2(\mu-NH)_2(\mu-Cl)]$ was crystallized and its crystal structure determined (CCDC 2080129)).

Reaction of **2 with excess HCl.** 200 μL of a 2M solution of HCl in Et_2O were added to **2** (11.3 mg, 0.0053 mmol, 1 equiv). The solution immediately turned light yellow. After 10 minutes, volatiles were removed under vacuum. The resultant solid was dissolved in 0.5 mL of d_6 -dmsO and dimethylsulfone was added as an internal standard for the quantitative NH_4Cl detection. NH_4Cl is formed in 93% yield.

Reaction of 4 with excess HCl. 300 μL of a 2M solution of HCl in Et_2O were added to **4** (6.2 mg, 0.0029 mmol, 1 equiv). The solution immediately turned light green. After 10 minutes, volatiles were removed under vacuum. The resultant solid was dissolved in 0.5 mL of d_6 -dmsd and dimethylsulfone was added as an internal standard for the quantitative NH_4Cl detection. NH_4Cl is formed in 100% yield.

NMR Spectra

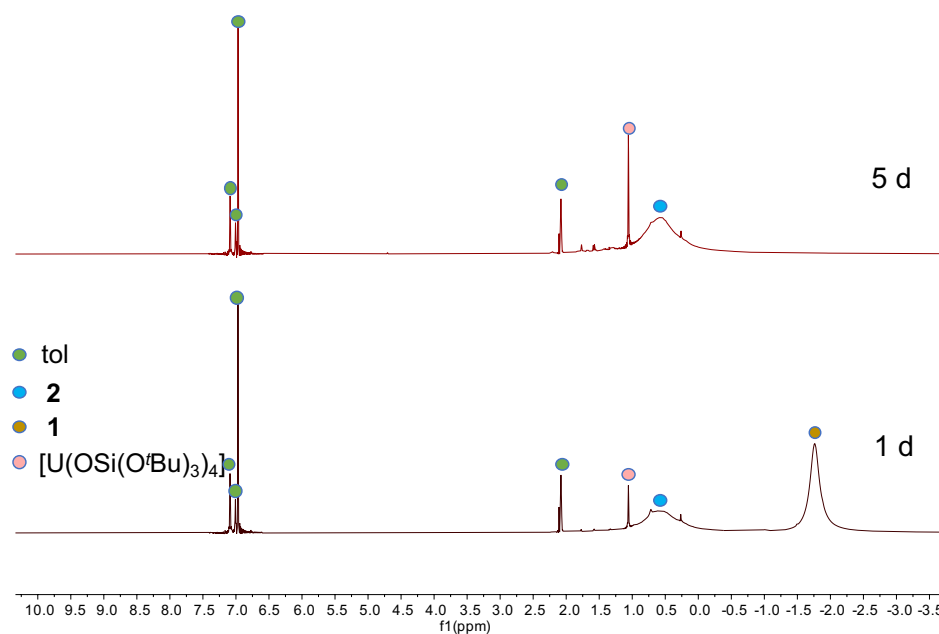


Figure S1. Evolution of the ¹H NMR spectrum (400 MHz, 298K, *d*₈-toluene) of the reaction mixture obtained 1 day (bottom) and 5 days (top) after the addition of 1 equiv of AgBPh₄ to **1**

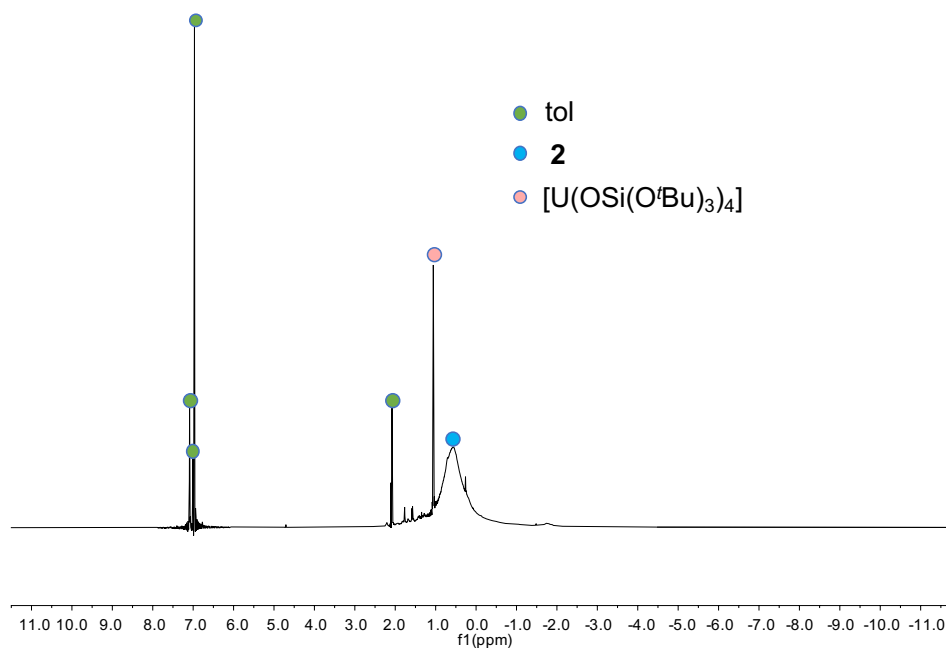


Figure S2. ¹H NMR spectrum (400 MHz, 298K, *d*₈-toluene) of the reaction between **1** and **2** equiv of AgBPh₄ overnight forming complex **2**

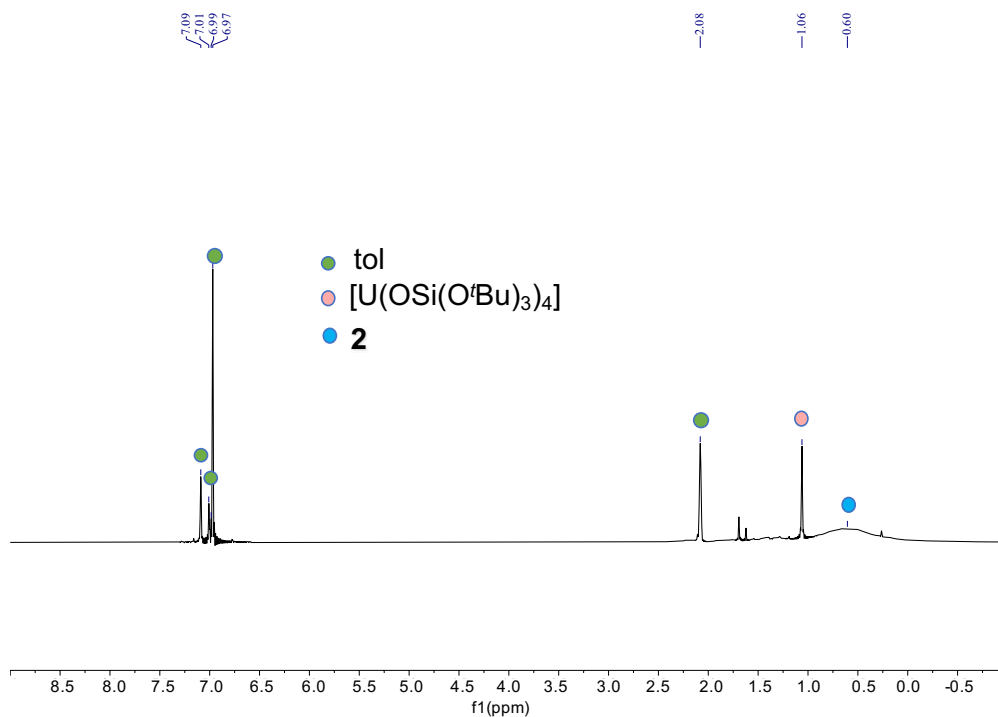


Figure S3. ^1H NMR spectrum (400 MHz, 298K, d_8 -toluene) of isolated complex **2**, isolated crystals may contain traces of the $[\text{U}(\text{OSi}(\text{O}^t\text{Bu})_3)_4]$ in 3-7% ratio compared to **2**.

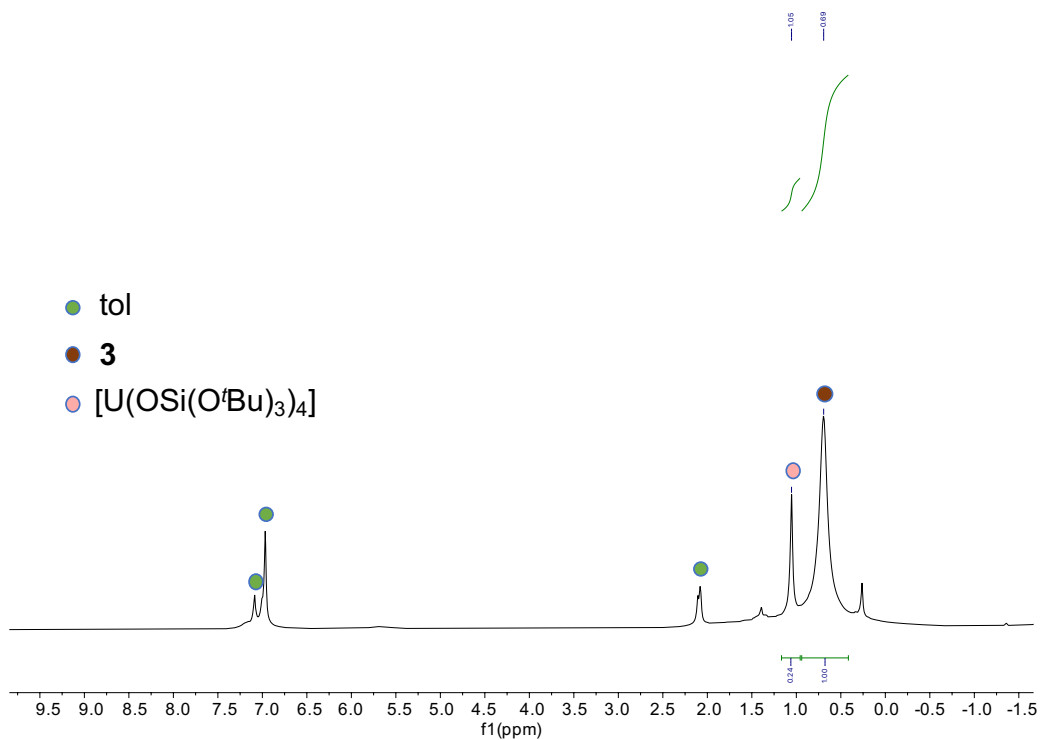


Figure S4. ^1H NMR spectrum (400 MHz, 298K, d_8 -toluene) immediately after addition of 0.5 equiv of I_2 to **1** yielding complex **3**

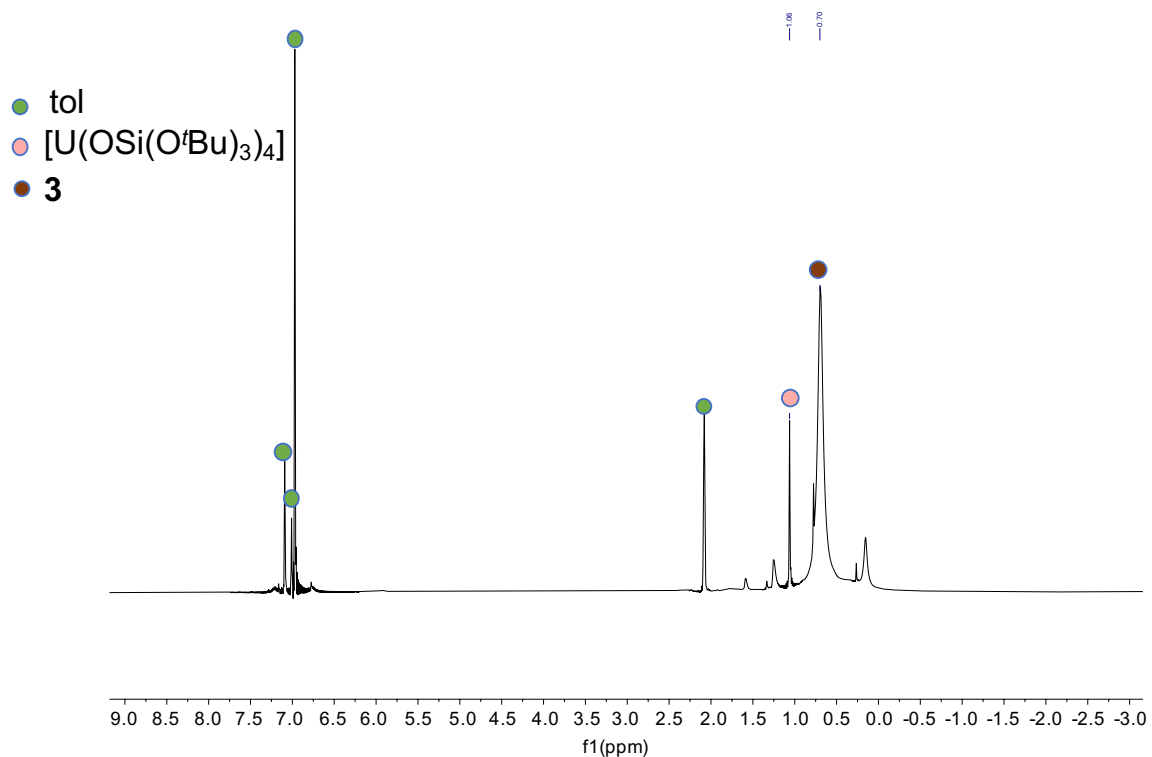


Figure S5. ¹H NMR spectrum (400 MHz, 298K, *d*₈-toluene) of **3**, isolated crystals always contain traces of the [U(OSi(O^tBu)₃)₄] complex.

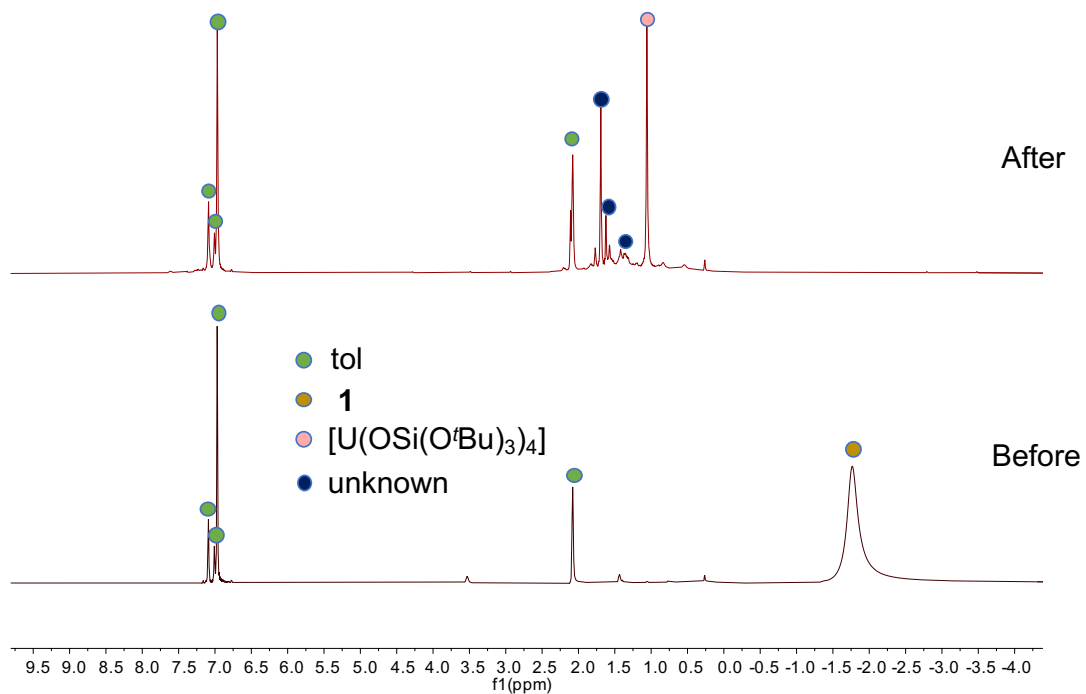


Figure S6. ¹H NMR spectra (400 MHz, 298K, *d*₈-toluene) before and after addition of 10 equiv of AgBPh₄ to **1**

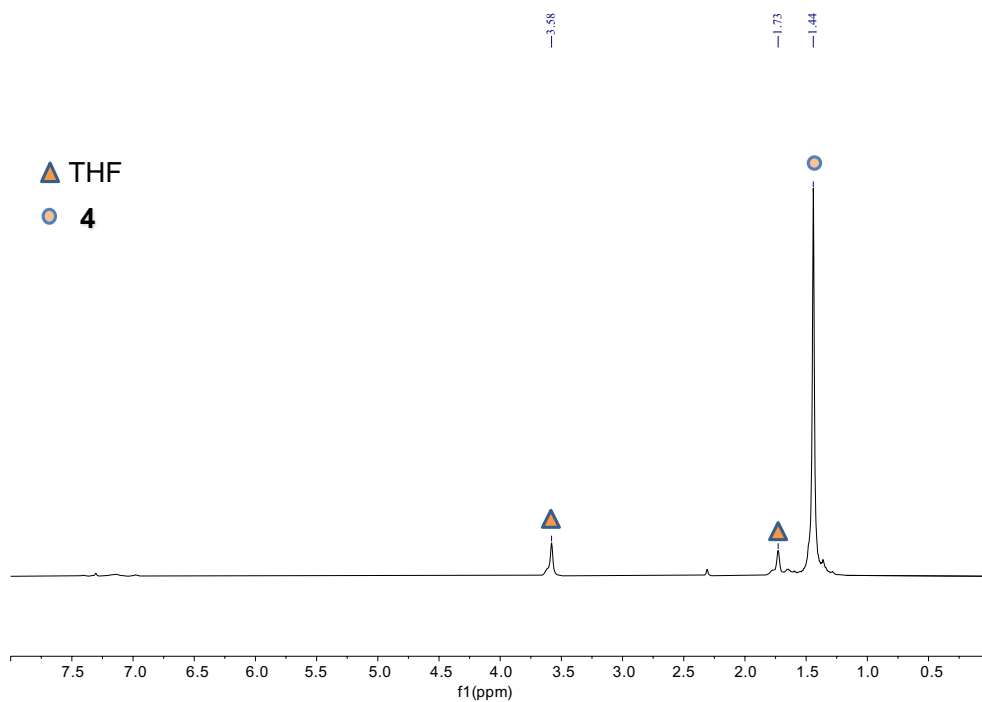


Figure S9. ^1H NMR spectrum (400 MHz, 298K, d_8 -thf) of isolated complex $[\{\text{U}(\text{OSi}(\text{O}^t\text{Bu})_3)_3\}_2(\mu\text{-N})_2(\mu\text{-thf})]$, **4**.

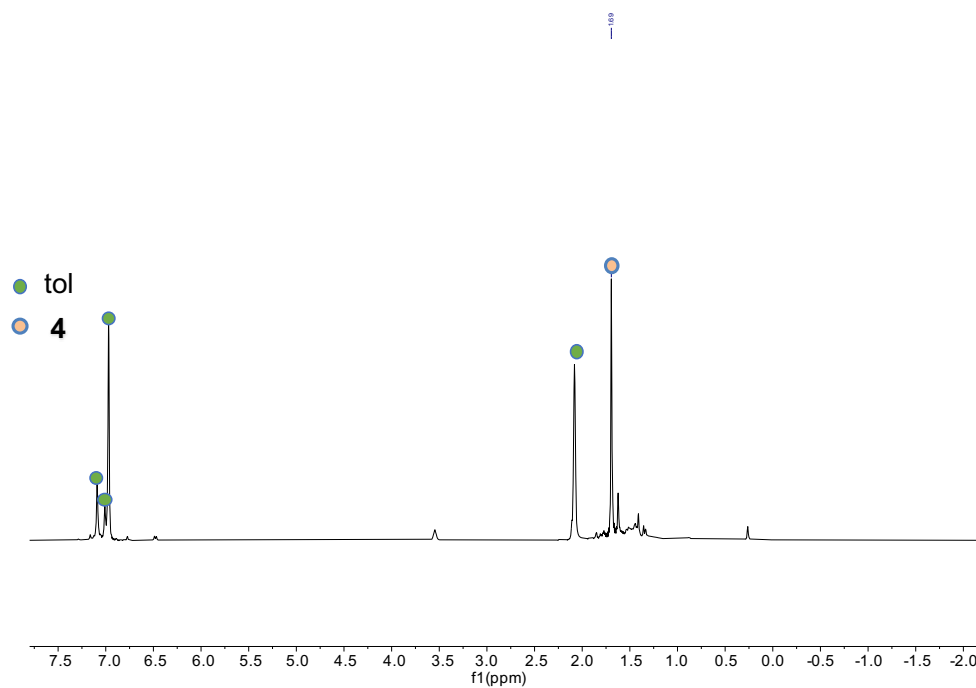


Figure S10. ^1H NMR spectrum (400 MHz, 298K, d_8 -toluene) of isolated complex $[\{\text{U}(\text{OSi}(\text{O}^t\text{Bu})_3)_3\}_2(\mu\text{-N})_2(\mu\text{-thf})]$, **4**

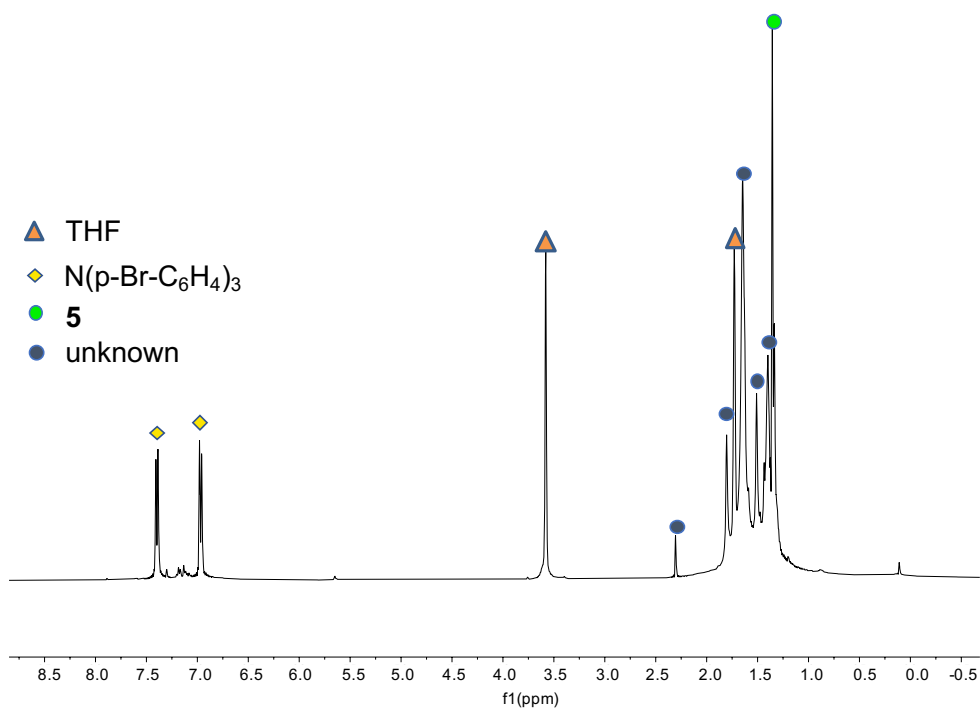


Figure S11. ¹H NMR spectrum (400 MHz, 298K, *d*₈-thf) of the residue obtained after solvent removal under vacuum from the reaction mixture between **1** and 2 equiv of [N(C₆H₄Br)₃][SbCl₆].

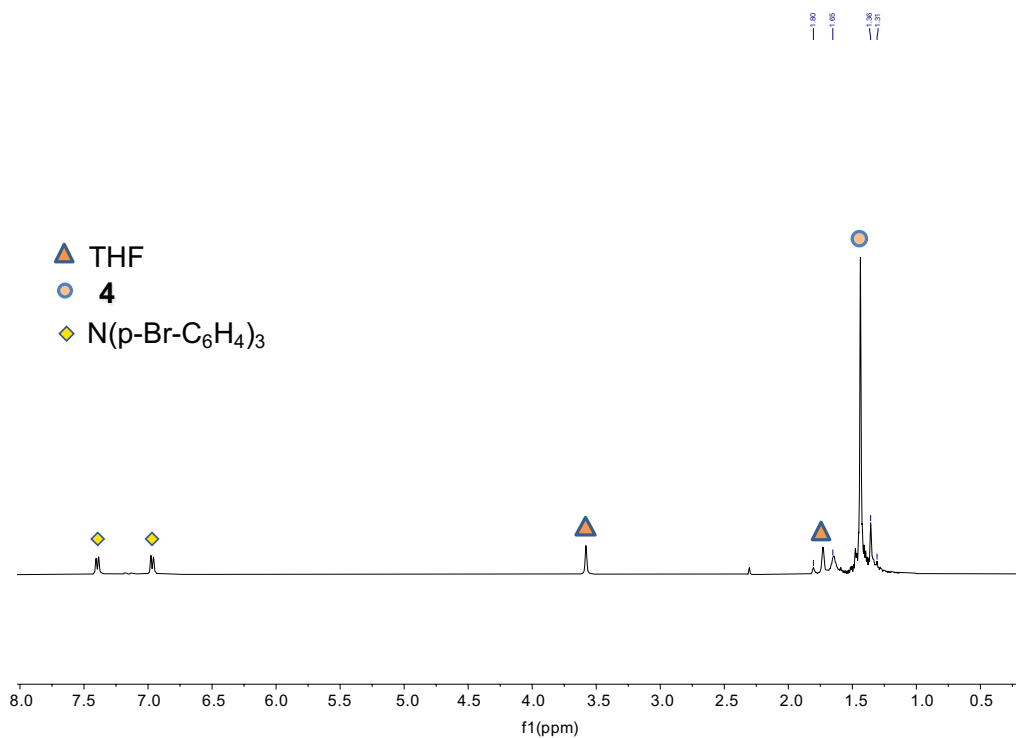


Figure S12. ¹H NMR spectrum (400 MHz, 298K, *d*₈-thf) of the residue obtained after solvent removal under vacuum at -80°C for 8h from the reaction mixture between **1** and 2 equiv of [N(C₆H₄Br)₃][SbCl₆].

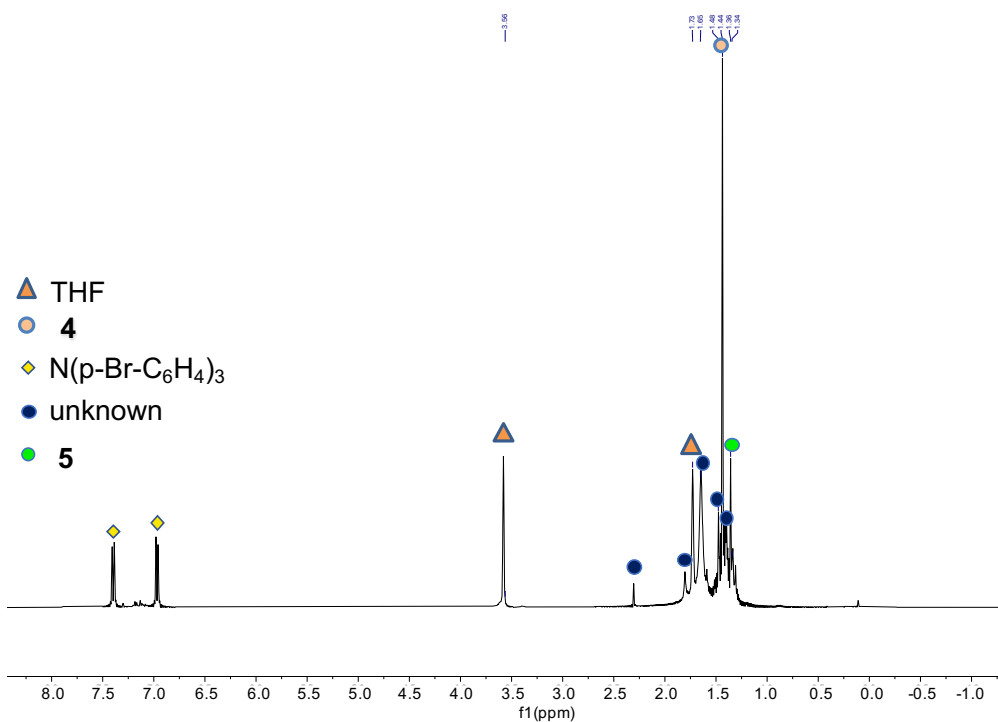


Figure S13. ^1H NMR spectrum (400 MHz, 298K, d_8 -thf) of the residue obtained after solvent removal under vacuum at -80°C for 12h from the reaction mixture between **1** and 2 equiv of $[\text{N}(\text{C}_6\text{H}_4\text{Br})_3][\text{SbCl}_6]$.

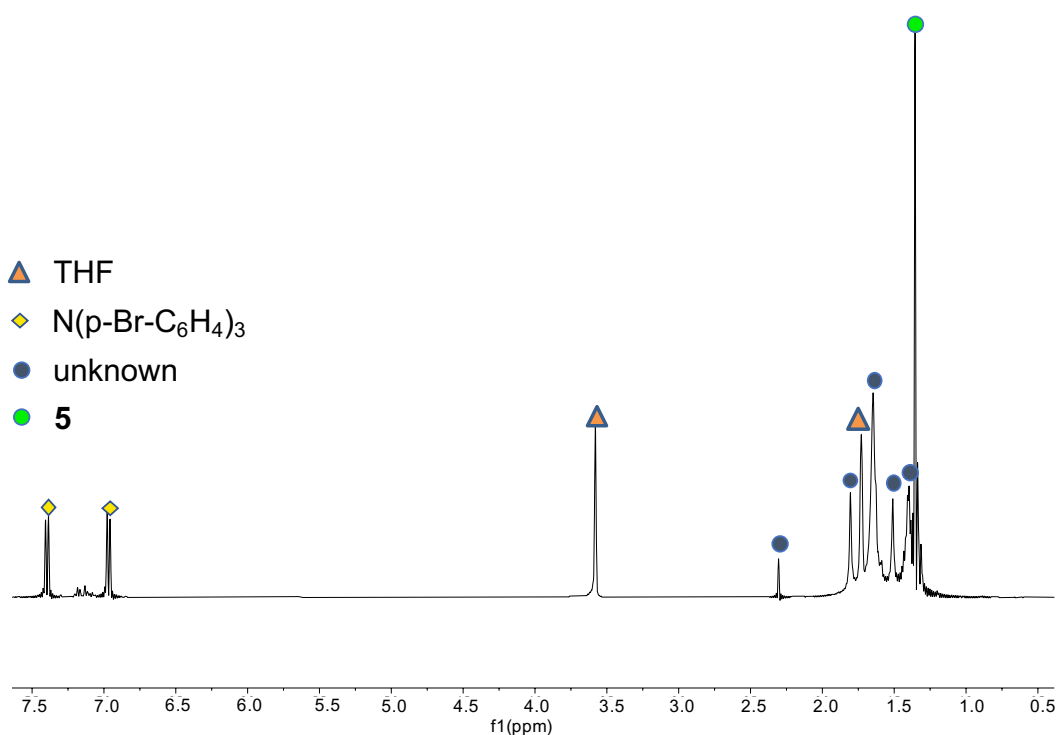


Figure S14. ^1H NMR spectrum (400 MHz, 298K, d_8 -thf) of the reaction mixture obtained after leaving reacting for 5 days at room temperature 2 equiv of $[\text{N}(\text{C}_6\text{H}_4\text{Br})_3][\text{SbCl}_6]$ to **1**.

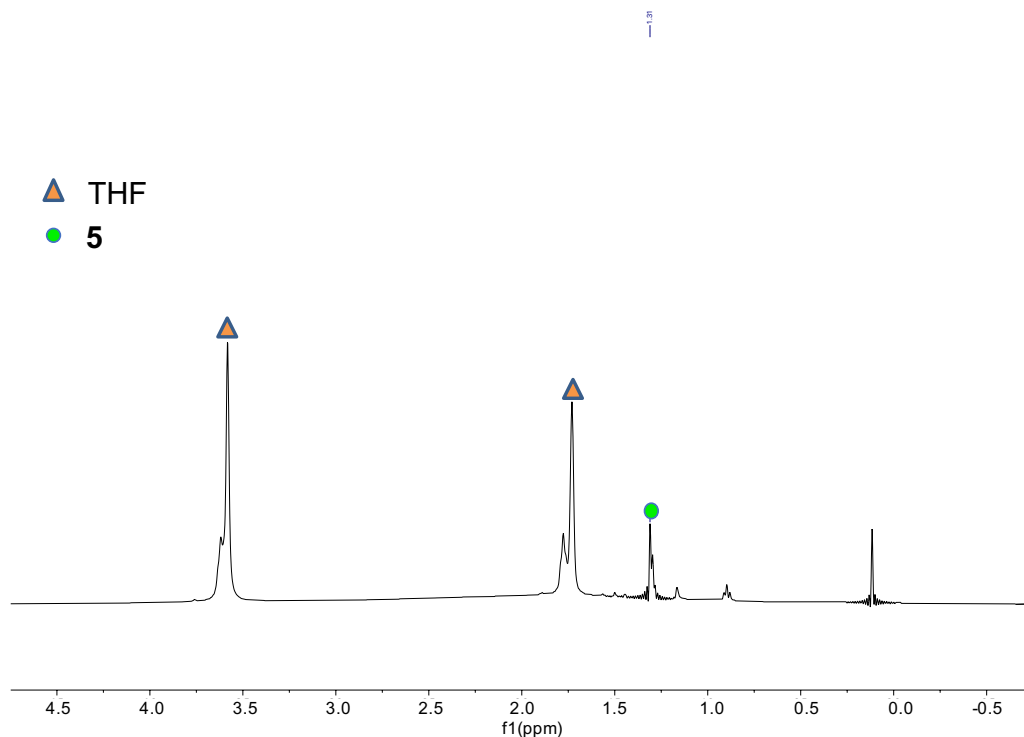


Figure S15. ^1H NMR spectrum (400 MHz, 298K, d_8 -thf) of isolated crystals of complex $[\text{U}(\text{OSi}(\text{OtBu})_3)_3\text{Cl}(\text{thf})_2]$, **5**

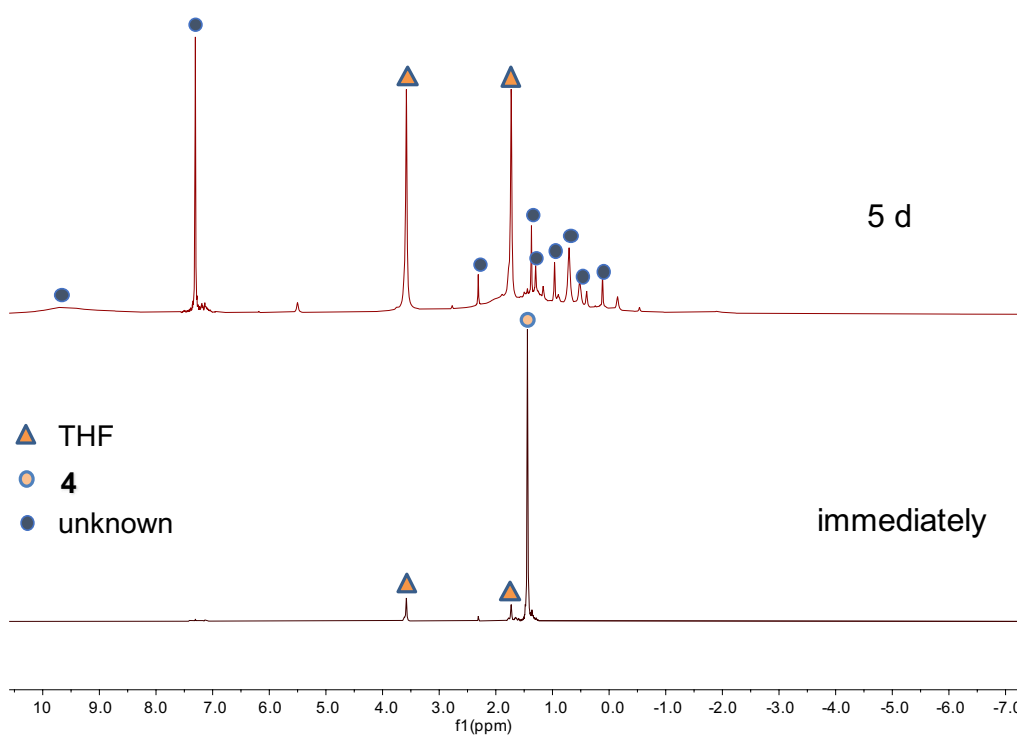


Figure S16. Evolution of the ^1H NMR spectrum (400 MHz, 298K, d_8 -thf) of isolated complex **4** under Ar showing complete disappearance of the signals of **4**.

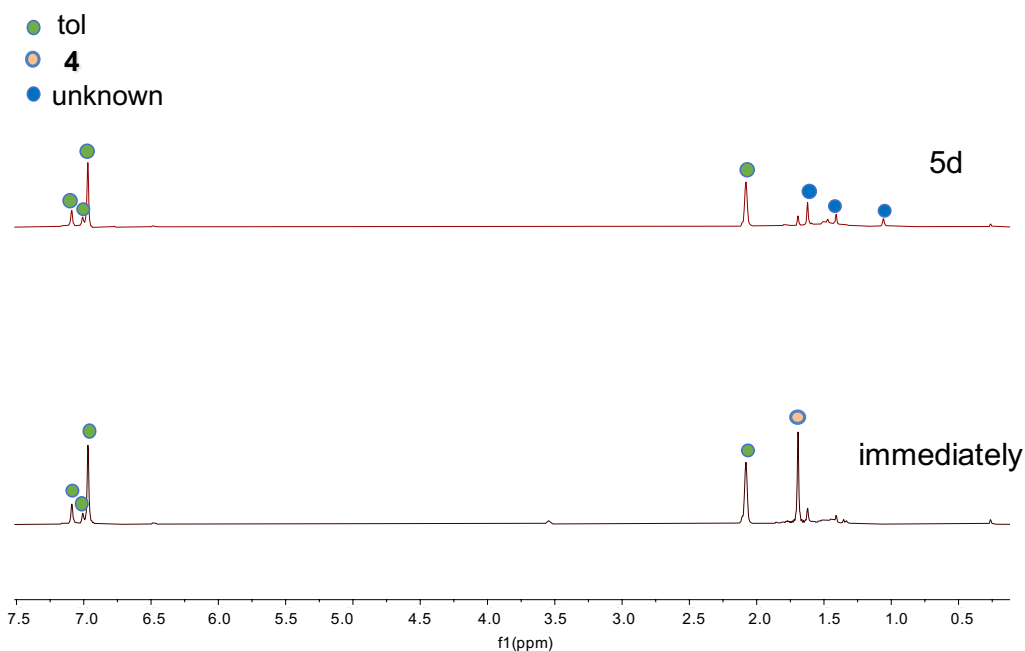


Figure S17. Evolution of the ^1H NMR spectrum (400 MHz, 298K, d_8 -toluene) of isolated complex **4** under argon showing complete disappearance of the signals of **4**.

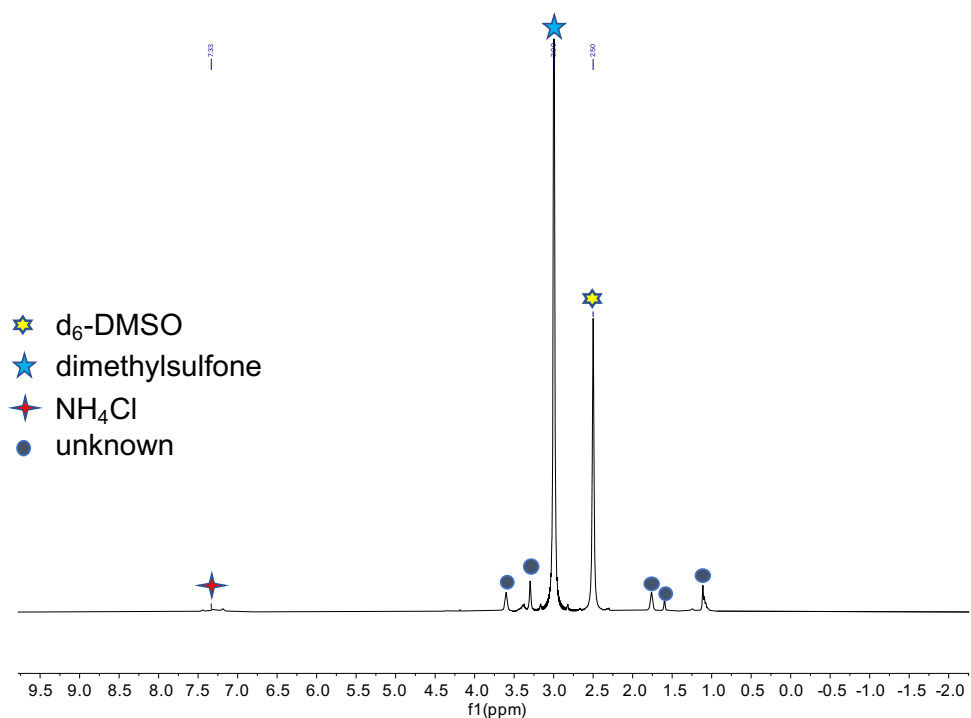


Figure S18. ^1H NMR spectrum (400 MHz, 298K, d_6 -dmsol) of the residue obtained after evaporation of the reaction mixture resulting from the decomposition under argon of isolated **4**, after addition of excess 2M HCl (Et_2O). The spectrum shows only traces of NH_4Cl .

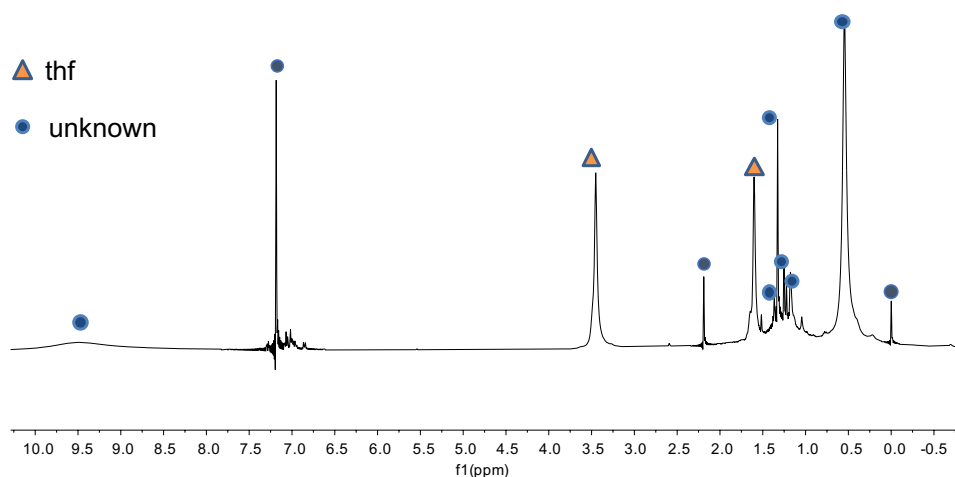


Figure S19. ^1H NMR spectrum (400 MHz, 298K, d_8 -thf) of isolated complex **4** after exposing the solid to dynamic vacuum for 15 minutes showing complete disappearance of the signals of **4**.

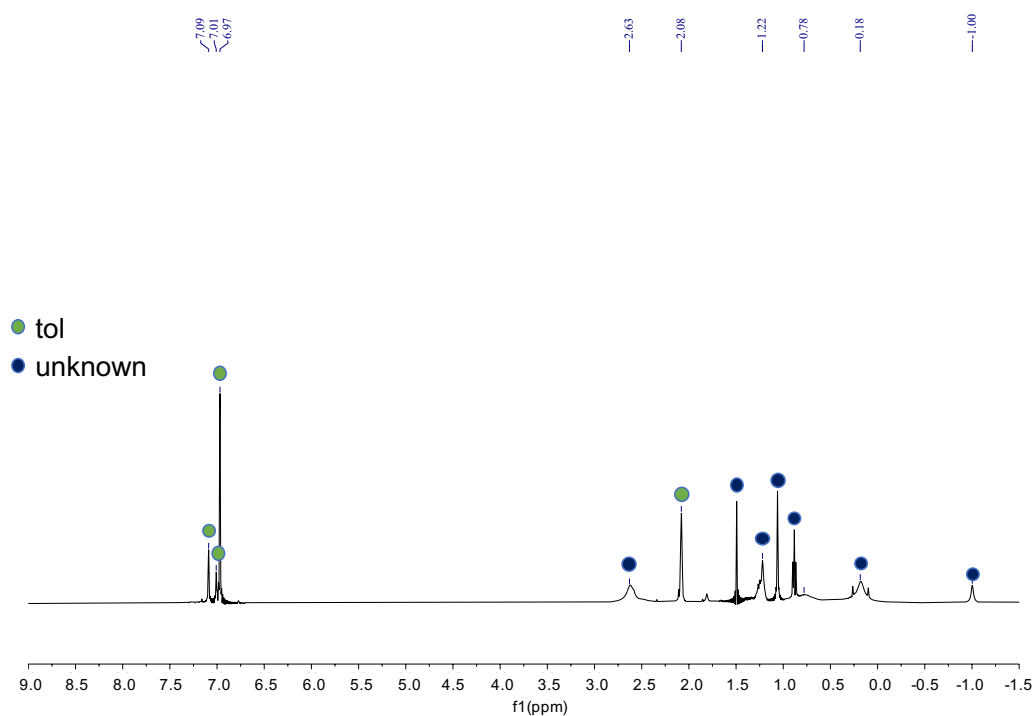


Figure S20. ^1H NMR spectrum (400 MHz, 298K, d_8 -toluene) of the reaction mixture between **2** and 1 atm of ^{13}C O.

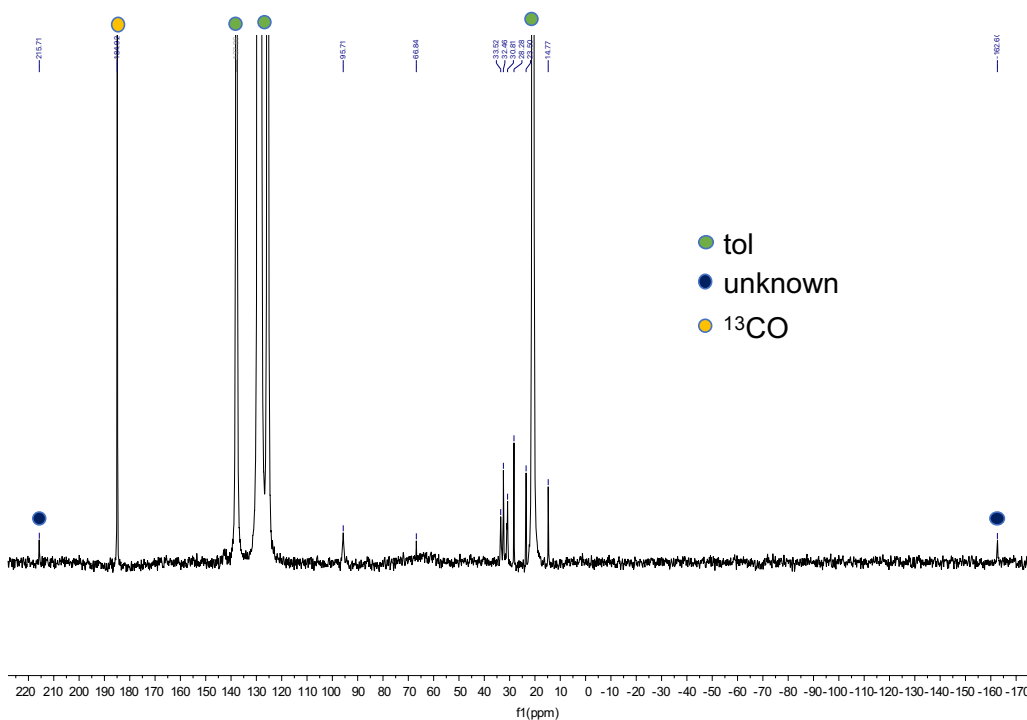


Figure S21. ¹³C NMR spectrum (151 MHz, 298K, *d*₈-toluene) of the reaction mixture between **2** and 1 atm of ¹³CO.

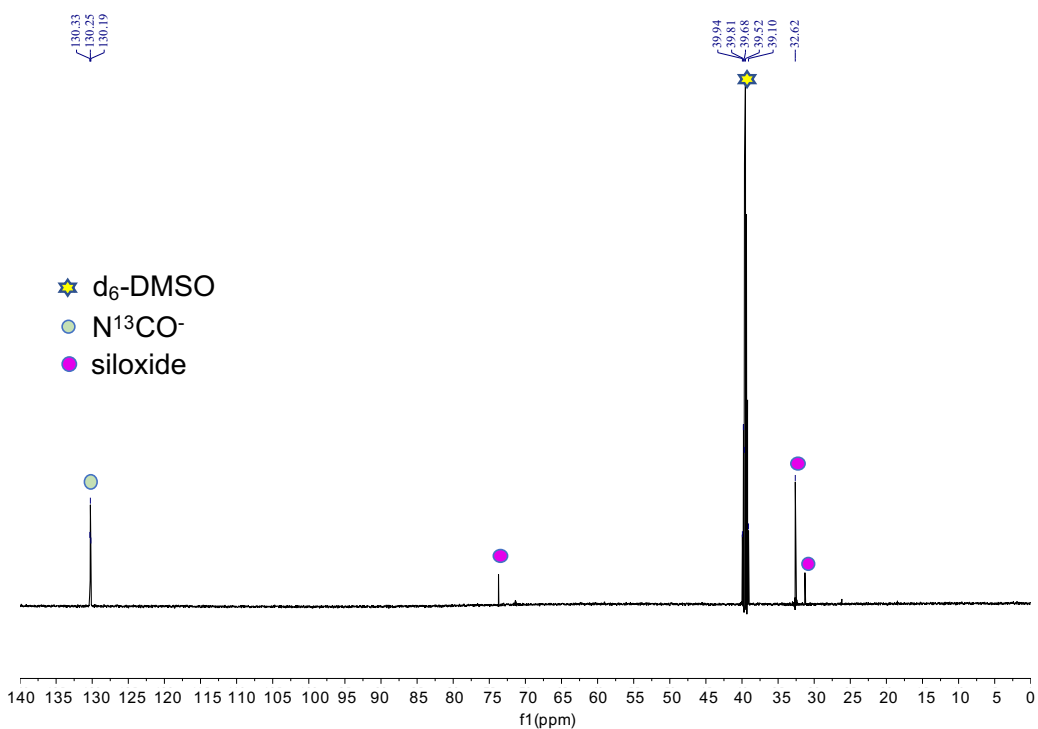


Figure S22. ¹³C NMR spectrum (151 MHz, 298K, D₂O) of the hydrolysis of the reaction mixture of **2** with ¹³CO in *d*₈-toluene with a pD = 12 D₂O solution.

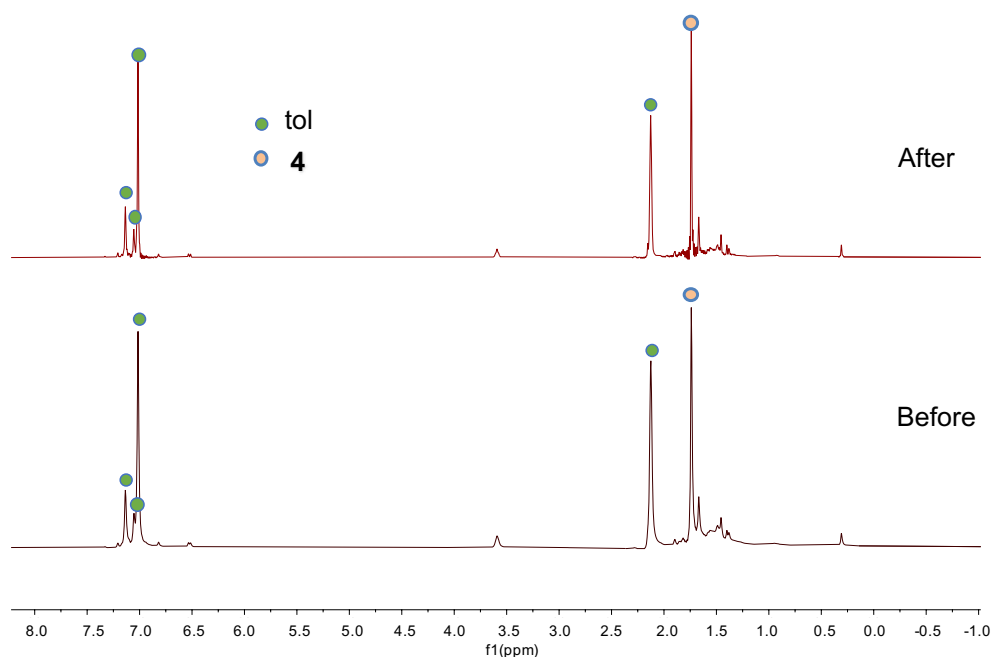


Figure S23. ^1H NMR spectra (400 MHz, 298K, d_8 -toluene) comparison between isolated complex **4** and the reaction mixture immediately after addition of ^{13}CO to isolated complex **4** showing absence of reaction.

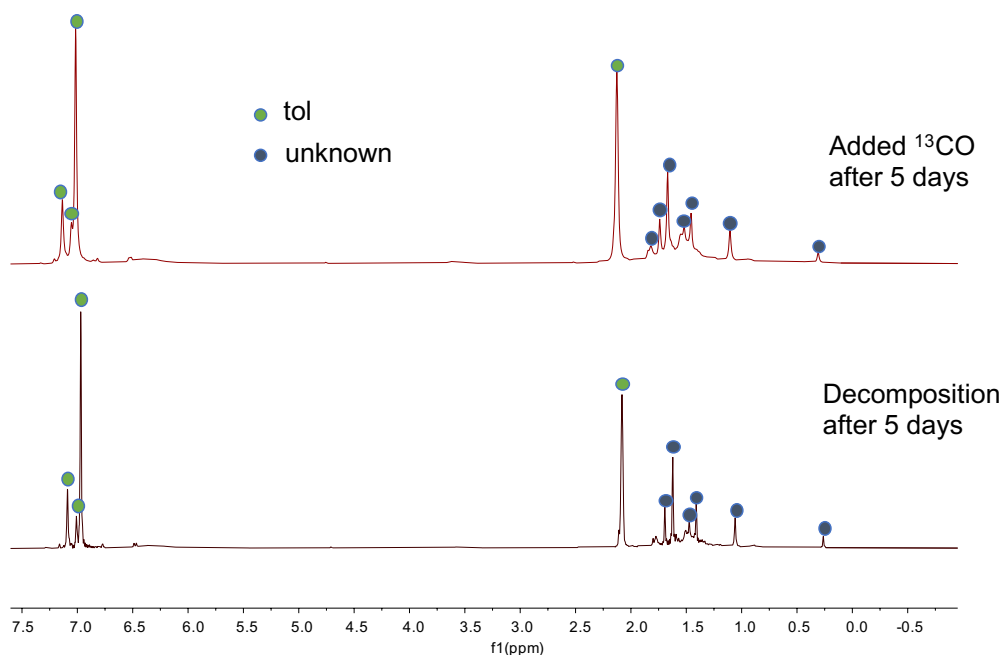


Figure S24. ^1H NMR spectra (400 MHz, 298K, d_8 -toluene) comparison between the decomposition of complex **4** under argon after 5 days and the reaction mixture 5 days after addition of ^{13}CO to isolated complex **4**.

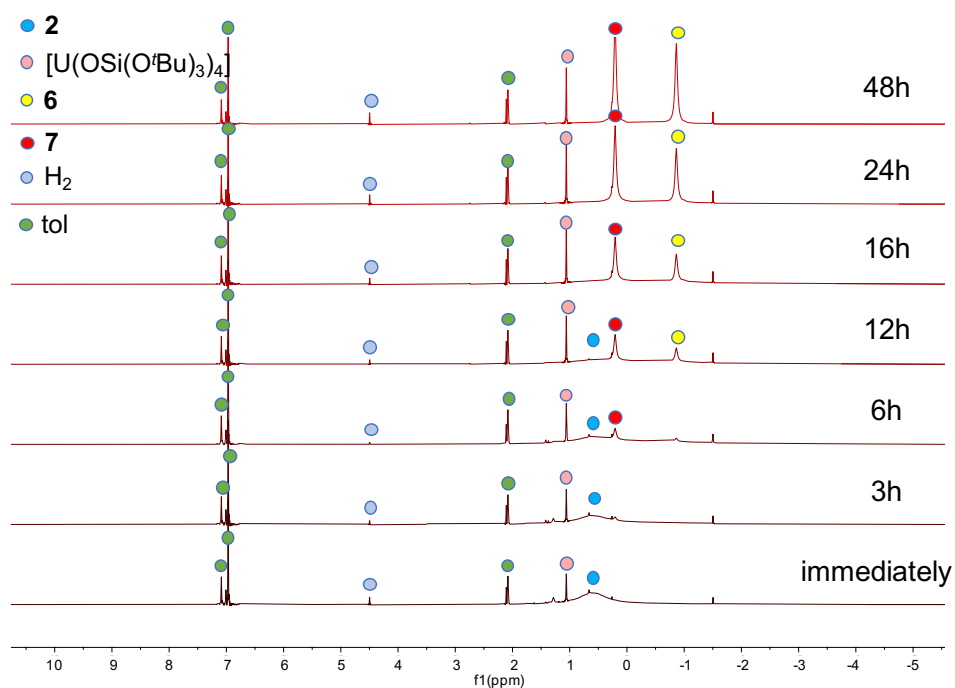


Figure S25. ^1H NMR spectra (400 MHz, 298K, d_8 -toluene) showing the evolution of the reaction mixture between complex **2** and 1 atm of H_2 forming the complexes **6** and **7**

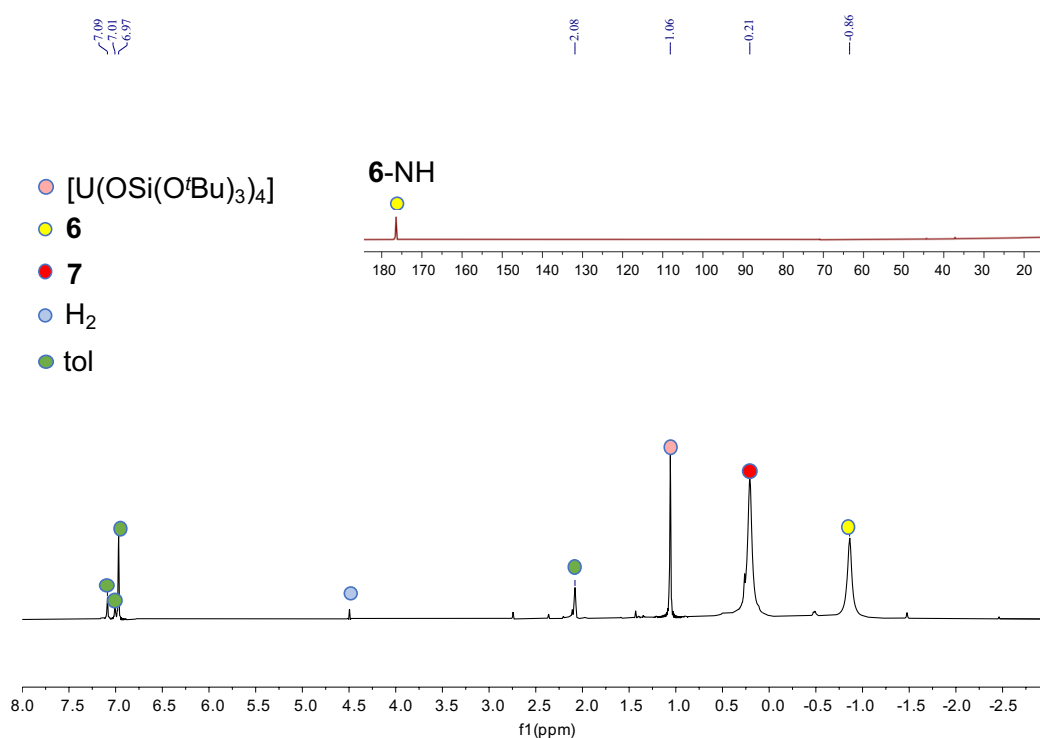


Figure S26. ^1H NMR spectrum (400 MHz, 298K, d_8 -toluene) of the reaction mixture between complex **2** and 1 atm of H_2 after 2d. The inset shows the peaks of the NH protons of **6**. The NH protons of the complex **7** could not be identified in d_8 -toluene.

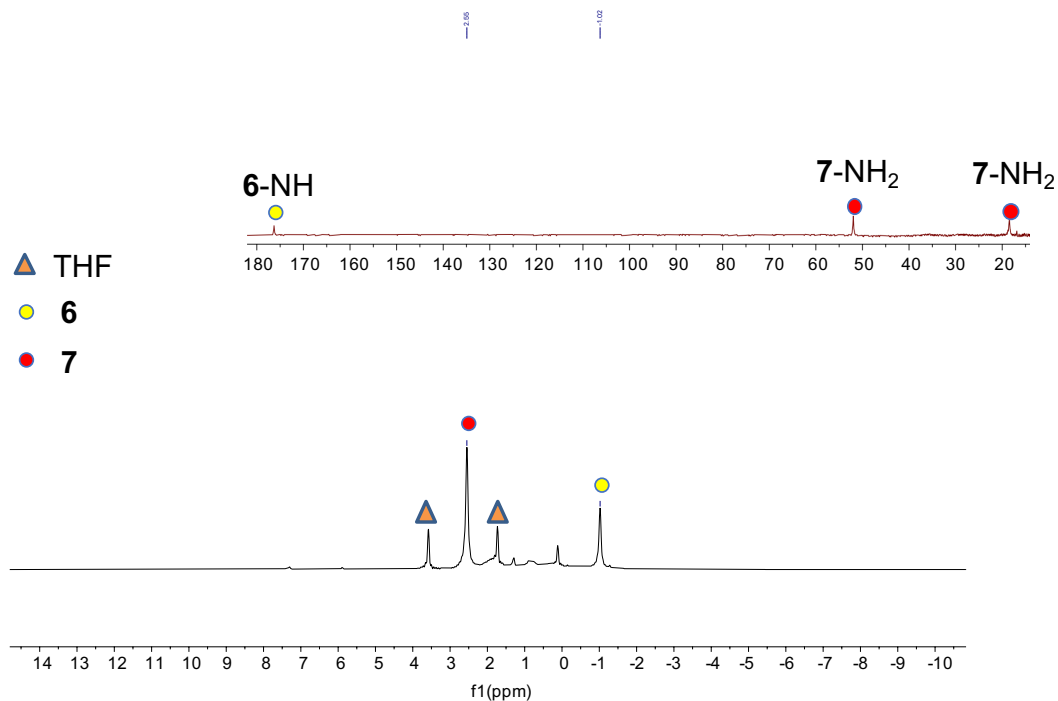


Figure S27. ¹H NMR spectrum (400 MHz, 298K, *d*₈-thf) of the reaction mixture between complex **2** and 1 atm of H₂ after 2d. The inset shows the peaks of the NH protons of **6** and **7**.

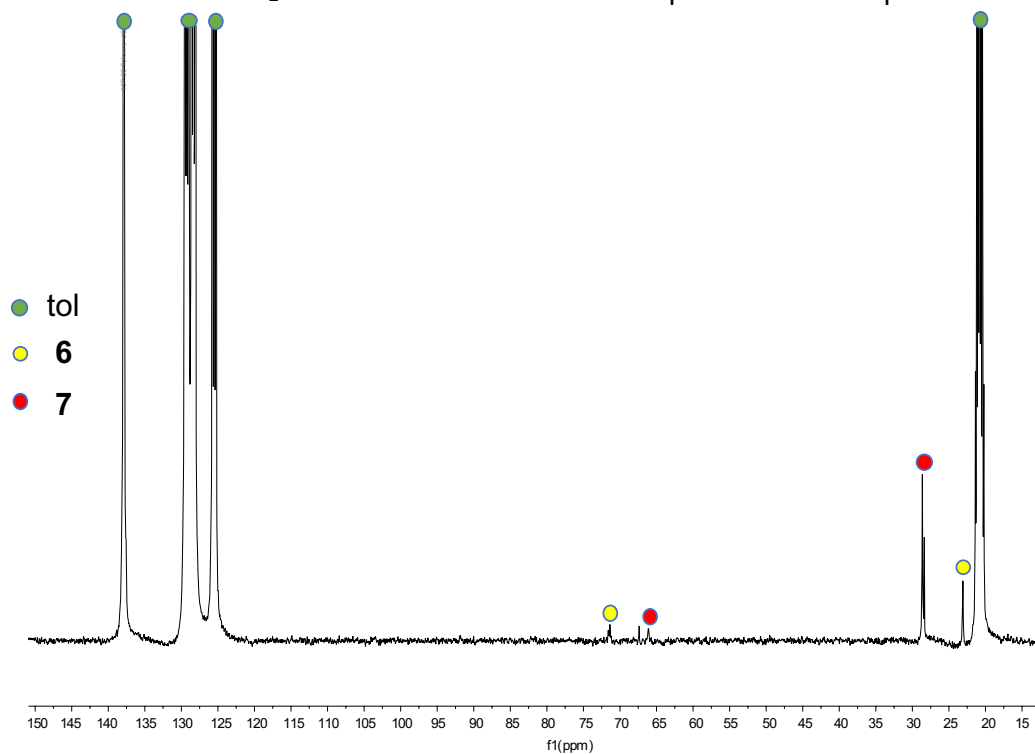


Figure S28. ¹³C NMR spectrum (100 MHz, 298K, *d*₈-toluene) of the reaction mixture between complex **2** and 1 atm of H₂ after 2d.

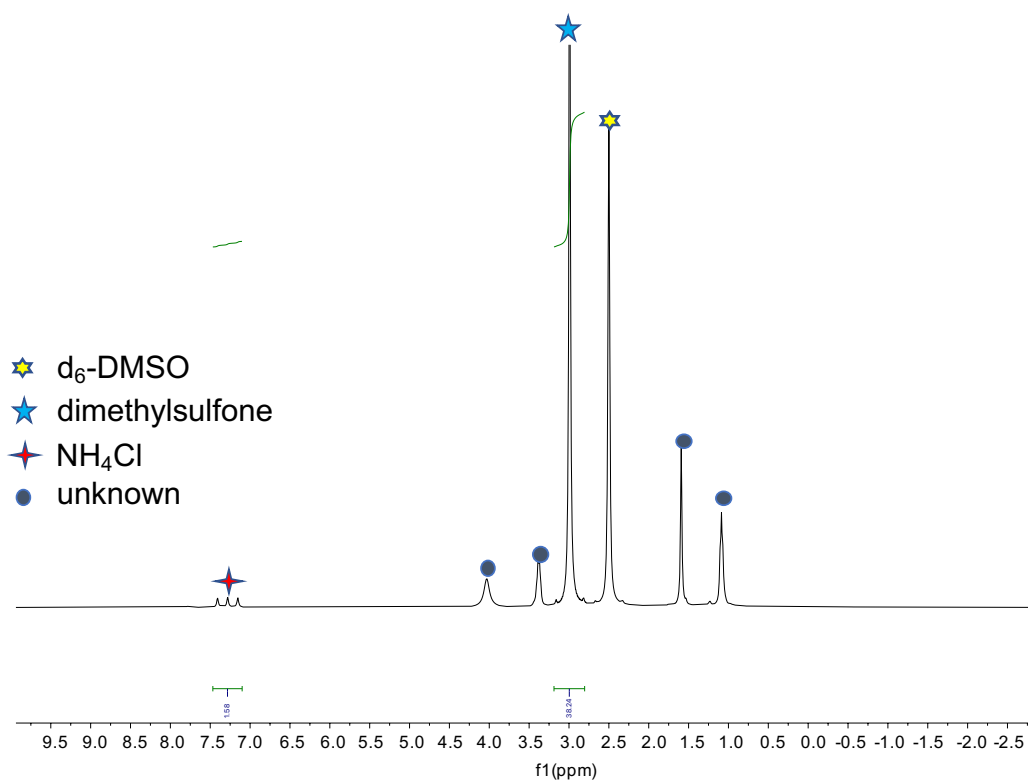


Figure S29. ¹H NMR spectrum (400 MHz, 298K, *d*₆-dmsol) after addition of excess 2M HCl (Et₂O) to the residue obtained after evaporation of the reaction mixture obtained after reacting **2** with 1 atm of H₂ for 2 days.

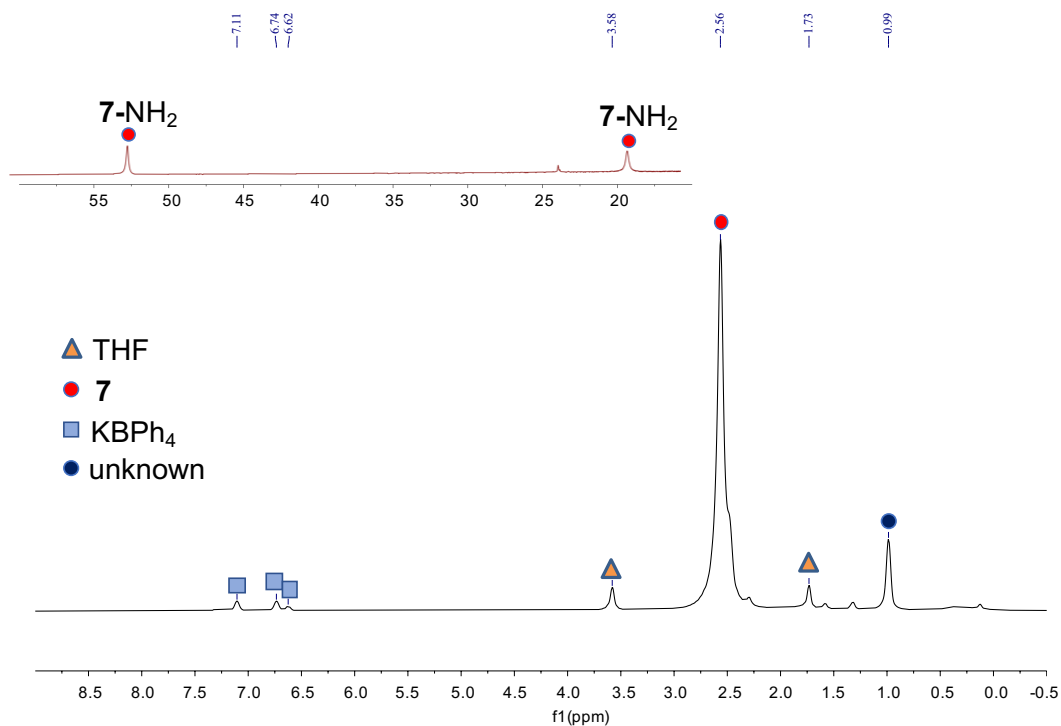


Figure S30. ¹H NMR spectrum (400 MHz, 298K, *d*₈-thf) of the reaction mixture between complex **6** and 2 equiv of NEt₃HBPh₄ forming complex **7**.

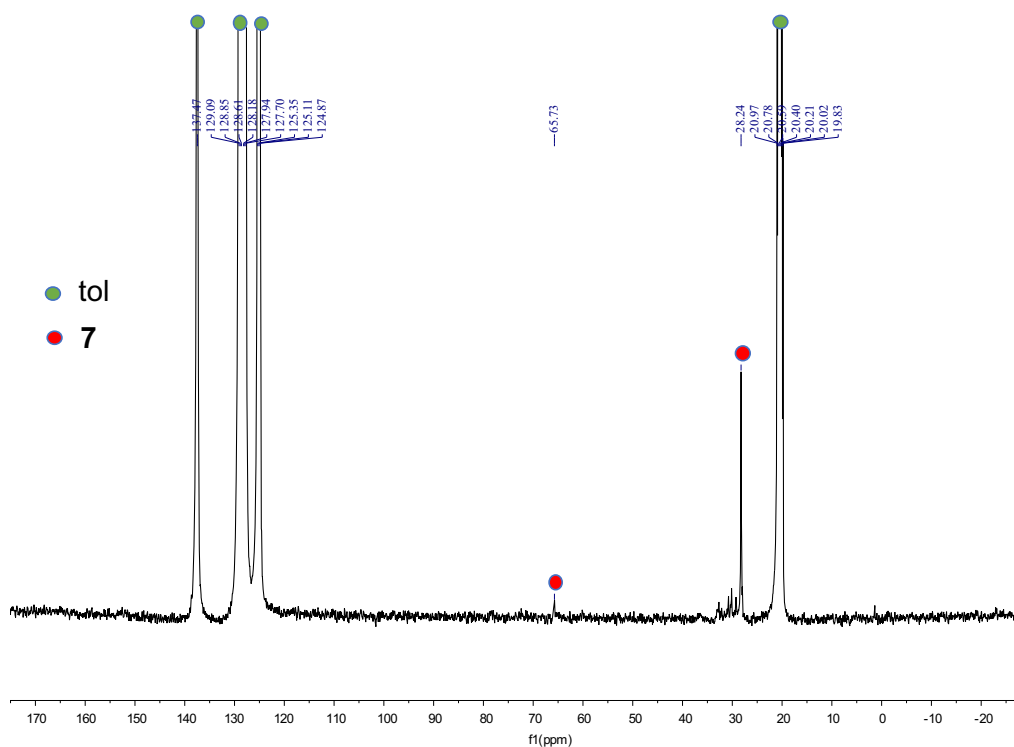


Figure S31. ^{13}C NMR spectrum (100 MHz, 298K, d_8 -toluene) of isolated complex **7**.

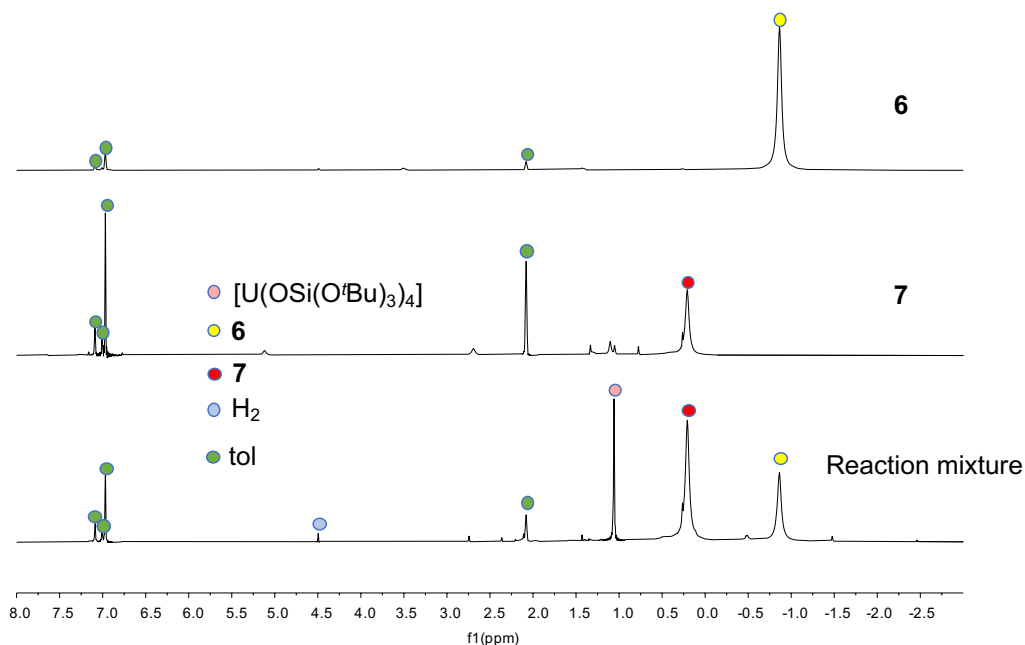


Figure S32. ^1H NMR spectra (400 MHz, 298K, d_8 -toluene) in the -3 to 8 ppm range of the reaction mixture obtained after reacting **2** with 1 atm of H_2 for 2 days (bottom), of the isolated complex **7** (middle), and of the isolated complex **6** (top).

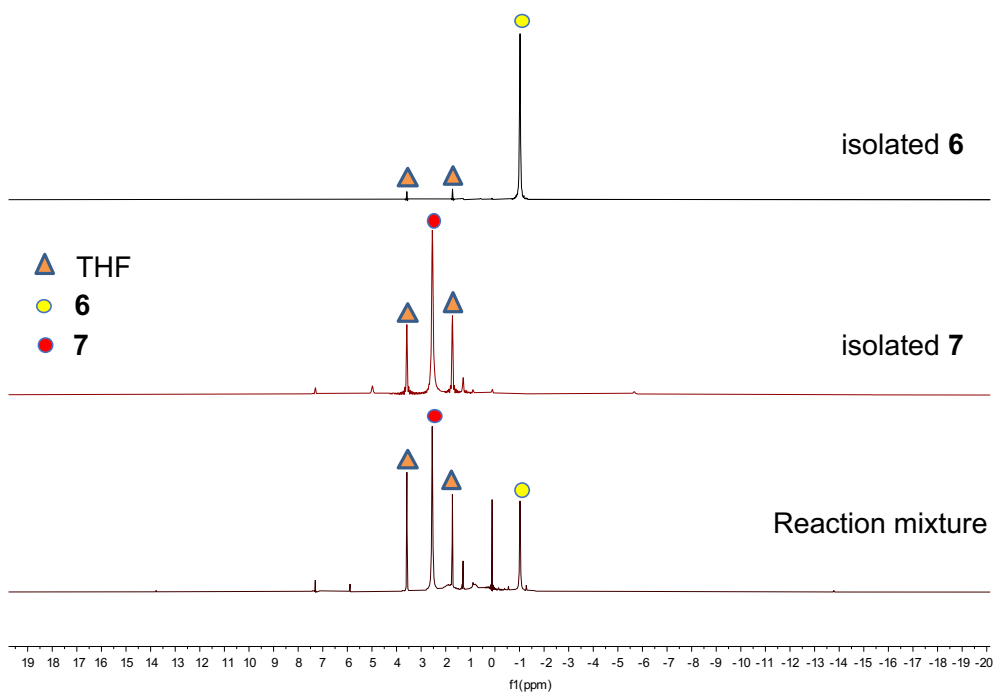


Figure S33. ^1H NMR spectra (400 MHz, 298K, d_8 -thf) (zoom in the 20 to -20 ppm range) of the reaction mixture obtained after reacting **2** with 1 atm of H_2 for 2 days (bottom), of the isolated complex **7** (middle), and of the isolated complex **6** (top).

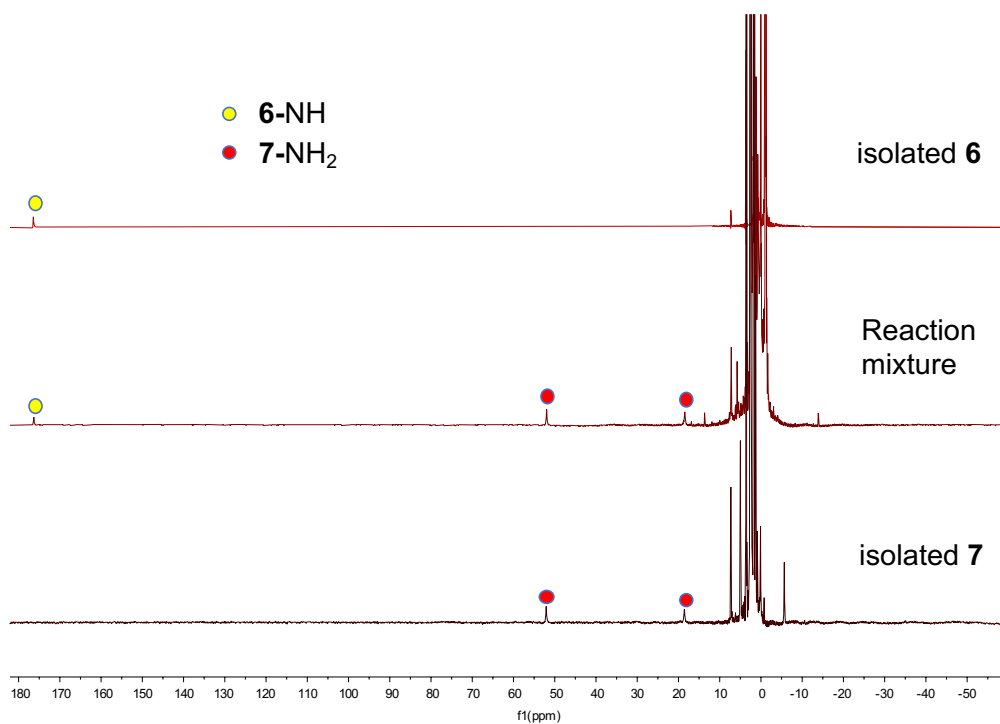


Figure S34. ^1H NMR spectra (400 MHz, 298K, d_8 -thf) of the reaction mixture obtained after reacting **2** with 1 atm of H_2 for 2 days (middle), of the isolated complex **7** (bottom), and of the isolated complex **6** (top).

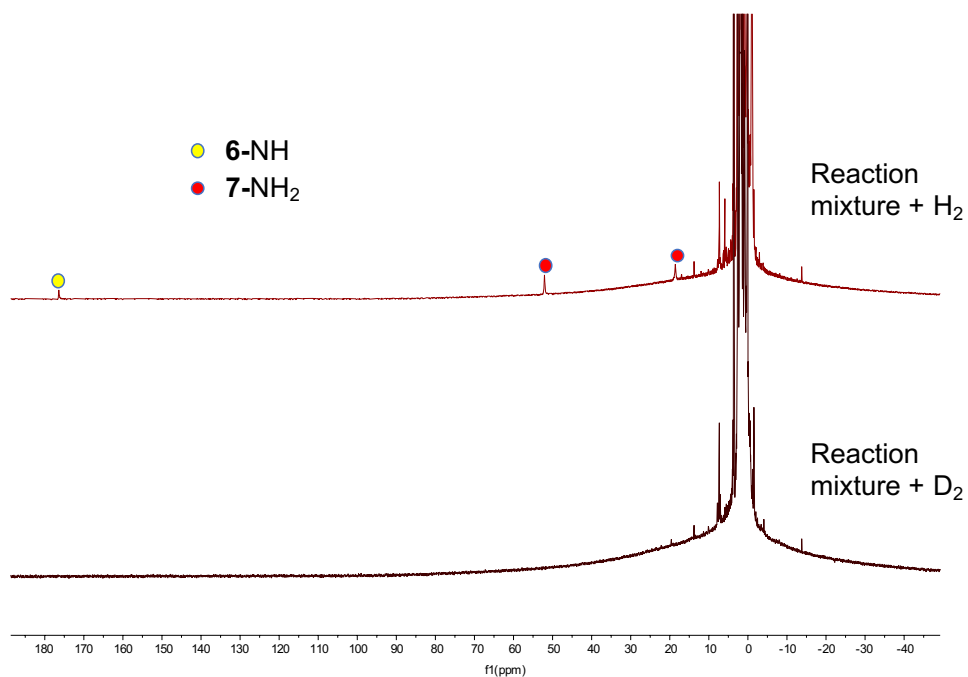


Figure S35. ^1H NMR spectra (400 MHz, 298K, d_8 -thf) of the reaction mixture between **2** + 1 atm of D_2 (bottom) and **2** + 1 atm of H_2 (top) after 2 days showing the disappearance of the NH and NH_2 signals .

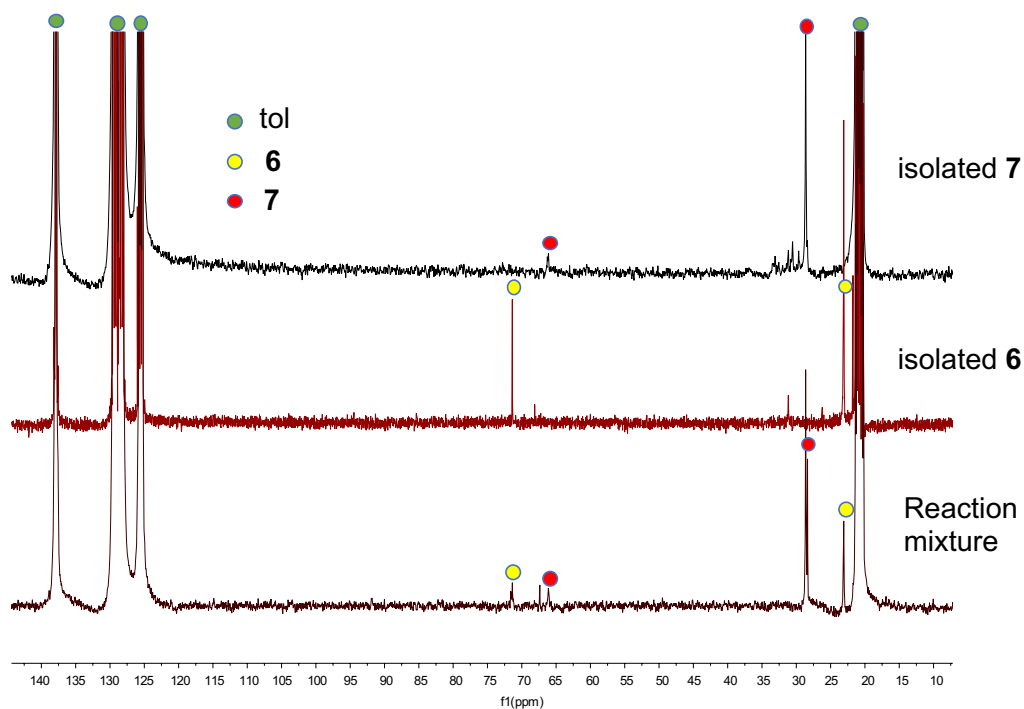


Figure S36. ^{13}C NMR spectra (100 MHz, 298K, d_8 -toluene) comparison of the reaction mixture between **2** and 1 atm of H_2 after 2 days, isolated complex **6**, and isolated complex **7**.

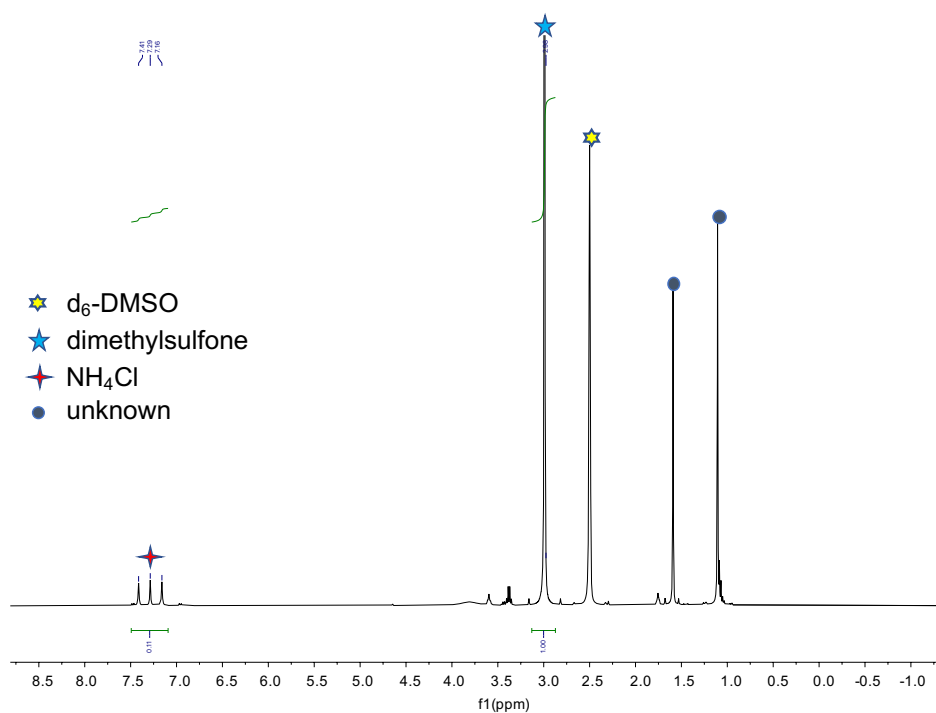


Figure S37. ¹H NMR spectrum (400 MHz, 298K, d₆-dmsO) of the residue after evaporation of the addition of excess 2M HCl (Et₂O) to isolated complex **4**

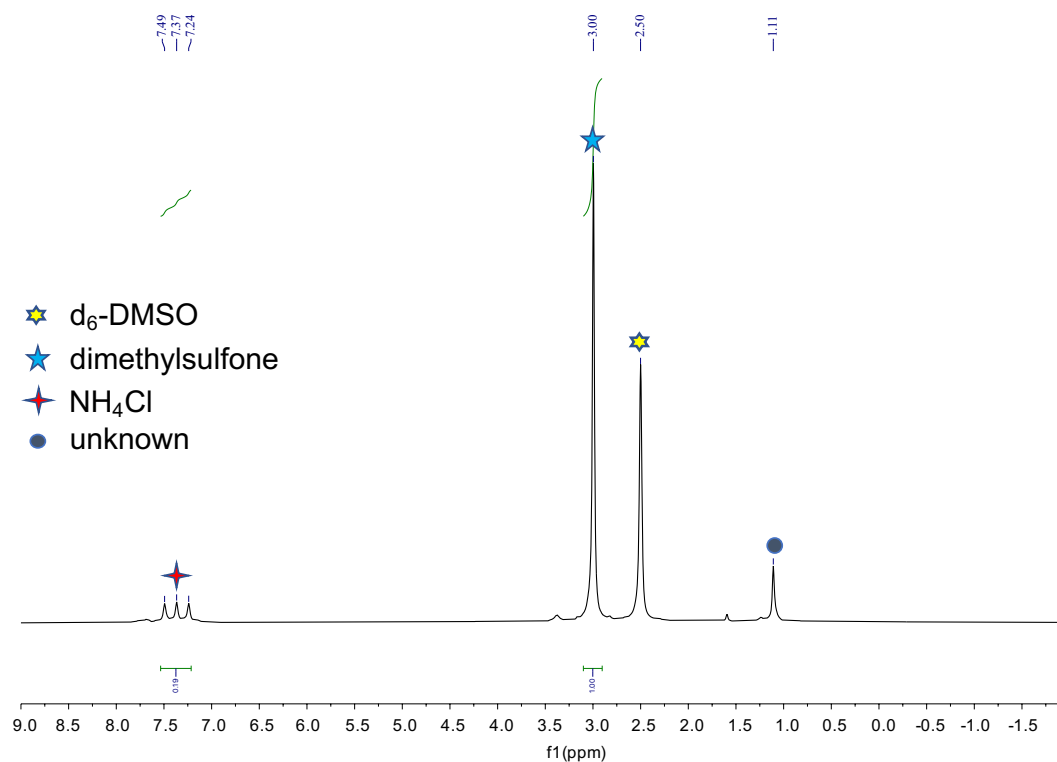


Figure S38. ¹H NMR spectrum (400 MHz, 298K, d₆-dmsO) of the residue after evaporation of the addition of excess 2M HCl (Et₂O) to isolated complex **2**

X-ray Crystallographic Details and Refinement Data

The diffraction data for the analysed crystal structures were collected at low temperature using Cu (**3**, **7**) or Mo (**2**, **4**, **5**) λ radiation on a Rigaku SuperNova dual system in combination with Atlas type CCD detector. The data reduction and correction were carried out by *CrysAlis^{Pro}*.⁴

The solutions and refinements were performed by *SHELXT*⁵ and *SHELXL*,⁶ respectively. The crystal structures were refined using full-matrix least-squares based on F^2 with all non-H atoms defined in anisotropic manner. Hydrogen atoms were placed in calculated positions by means of the “riding” model.

All compounds displayed disordered ligands. The extent of disorder involved the entire ligand or part of it. Several restraints were needed to model the geometry and displacement atomic parameters of the different orientations. In the case of compound **3**, the 2 nitrides and iodine are disordered over three positions and some strict restraints and constraints have been employed to adjust their occupancies, bond distances and ellipsoids. Due to the high degree of disorder, the free solvent molecules (toluene or THF) were removed in all crystal structures except **7** by applying the *SQUEEZE* algorithm of *PLATON*.⁷

Table S1. Crystal data and structural refinement parameters for complexes [K{U(OSi(O^tBu)₃)₃(μ-N)}₂], **2**, [K₂{U(OSi(O^tBu)₃)₃}₂(μ-N)₂(μ-I)], **3**, and [{U(OSi(O^tBu)₃)₃}₂(μ-N)₂(μ-thf)], **4**

	2	3	4
Formula	C ₇₂ H ₁₆₂ KN ₂ O ₂₄ Si ₆ U ₂	C ₇₂ H ₁₆₂ IK ₂ N ₂ O ₂₄ Si ₆ U ₂	C ₇₆ H ₁₇₀ N ₂ O ₂₅ Si ₆ U ₂
Crystal size (mm)	0.50×0.29×0.14	0.39×0.05×0.05	0.83×0.67×0.56
Crystal System	triclinic	monoclinic	monoclinic
Space Group	<i>P</i> -1	<i>P</i> 2 ₁	<i>P</i> 2 ₁
Volume (Å ³)	5561.21(18)	5571.5(2)	5508.59(17)
a (Å)	13.4396(3)	13.9014(3)	14.1108(3)
b (Å)	17.7067(3)	18.1586(5)	17.5538(3)
c (Å)	25.0094(5)	22.0984(5)	22.2467(4)
α (°)	80.0596(15)	90	90
β (°)	88.3887(15)	92.822(2)	91.4964(17)
γ (°)	71.6290(16)	90	90
Z	2	2	2
Formula Weight	2123.73	2289.80	2156.73
Density (g cm ⁻³)	1.268	1.365	1.300
μ (mm ⁻¹)	3.066	12.045	3.060
F(000)	2174	2318	2216
Temperature (K)	140.00(10)	140.00(10)	140.00(10)
Total Reflections	62738	107607	78955
Unique Reflections	26553	21762	22528
R _{int}	0.0319	0.0698	0.0467
R Indices [I > 2σ(I)]	R ₁ = 0.0461 wR ₂ = 0.1071	R ₁ = 0.0481 wR ₂ = 0.1200	R ₁ = 0.0697 wR ₂ = 0.1877
Largest Diff. Peak and Hole (e.Å ⁻³)	4.664 and -1.598	1.693 and -1.328	5.384 and -1.371
GOF	1.036	1.043	1.014

F(000), structure factor evaluated in the zeroth-order case, h=k=l= 0; R(int) = $\sum |F_o2 - F_o2(\text{mean})| / \sum [F_o2]$; I, measured intensities; 'Largest diff. peak and hole', maximum and minimum electron density found in the final Fourier difference map; GOF, goodness of fit (= $\{\sum [w(F_o2 - F_c2)^2] / (n-p)\}^{1/2}$, where n is the number of reflections and p is the total number of parameters refined).

Table S2. Crystal data and structural refinement parameters for complexes [U(OSi(O^tBu)₃)₃Cl(thf)₂], **5** and [U(OSi(O^tBu)₃)₃]₂(μ-NH₂)₂], **7**

	5	7
Formula	C ₄₄ H ₉₇ ClO ₁₄ Si ₃ U	C ₈₀ H ₁₈₄ N ₂ O ₂₆ Si ₆ U ₂
Crystal size (mm)	0.66×0.48×0.36	0.35×0.25×0.21
Crystal System	monoclinic	monoclinic
Space Group	<i>Cc</i>	<i>P2</i> ₁
Volume (Å ³)	12855.6(2)	5594.49(9)
a (Å)	24.6881(3)	14.34057(14)
b (Å)	14.15493(12)	17.69858(18)
c (Å)	38.5283(4)	22.05000(18)
α (°)	90	90
β (°)	107.2905(11)	91.5214(8)
γ (°)	90	90
Z	8	2
Formula Weight	1207.96	2234.88
Density (g cm ⁻³)	1.248	1.327
μ (mm ⁻¹)	2.671	9.201
F(000)	4992	2308
Temperature (K)	140.00(10)	140.00(10)
Total Reflections	166080	69237
Unique Reflections	43877	22639
R _{int}	0.0489	0.0346
R Indices [<i>I</i> > 2σ(<i>I</i>)]	R ₁ = 0.0455 wR ₂ = 0.0997	R ₁ = 0.0382 wR ₂ = 0.0940
Largest Diff. Peak and Hole (e.Å ⁻³)	1.462 and -2.753	2.016 and -2.307
GOF	1.057	1.022

F(000), structure factor evaluated in the zeroth-order case, h=k=l= 0; R(int) = $\sum |F_o2 - F_o2(\text{mean})| / \sum [F_o2]$; I, measured intensities; 'Largest diff. peak and hole', maximum and minimum electron density found in the final Fourier difference map; GOF, goodness of fit ($= \{\sum [w(F_o2 - F_c2)^2] / (n-p)\}^{1/2}$, where n is the number of reflections and p is the total number of parameters refined).

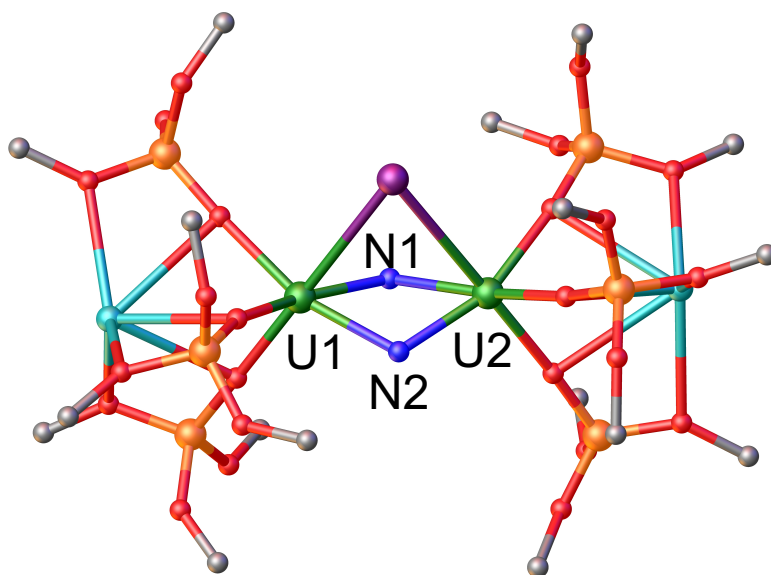


Figure S39. Molecular structure of $[K_2\{U(OSi(O^tBu)_3)_2(\mu-N)_2(\mu-I)\}]_2$, **3**, with thermal ellipsoids drawn at the 50% probability level. Hydrogen atoms and two molecules of toluene have been omitted for clarity. The two nitrogen and the iodine atoms in the core are disordered over three positions each. Only one position is shown for clarity. The average U-I distance is of 3.197(1) Å.

Structural description of complex 5

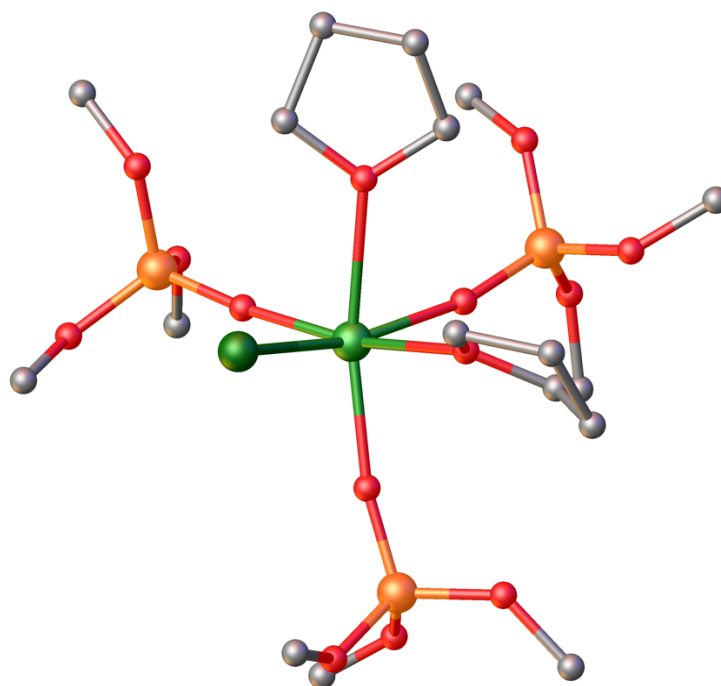


Figure S40. Molecular structure of $[\text{U}(\text{OSi}(\text{O}^t\text{Bu})_3)_2\text{Cl}(\text{thf})_2]$, **5**, with thermal ellipsoids drawn at the 50% probability level. Hydrogen atoms and two molecules of toluene have been omitted for clarity.

The molecular structure of the complex $[\text{U}(\text{OSi}(\text{O}^t\text{Bu})_3)_2\text{Cl}(\text{thf})_2]$, **5** shows a monomeric U(IV) complex. The U centre is hexacoordinated in a distorted octahedral geometry and is bound to three siloxide, two thf, and one chloride ligand. The average U-O_{sil} distance is of 2.14(1) Å and the U-Cl bond average distance is of 2.694(2) Å.

IR Spectra

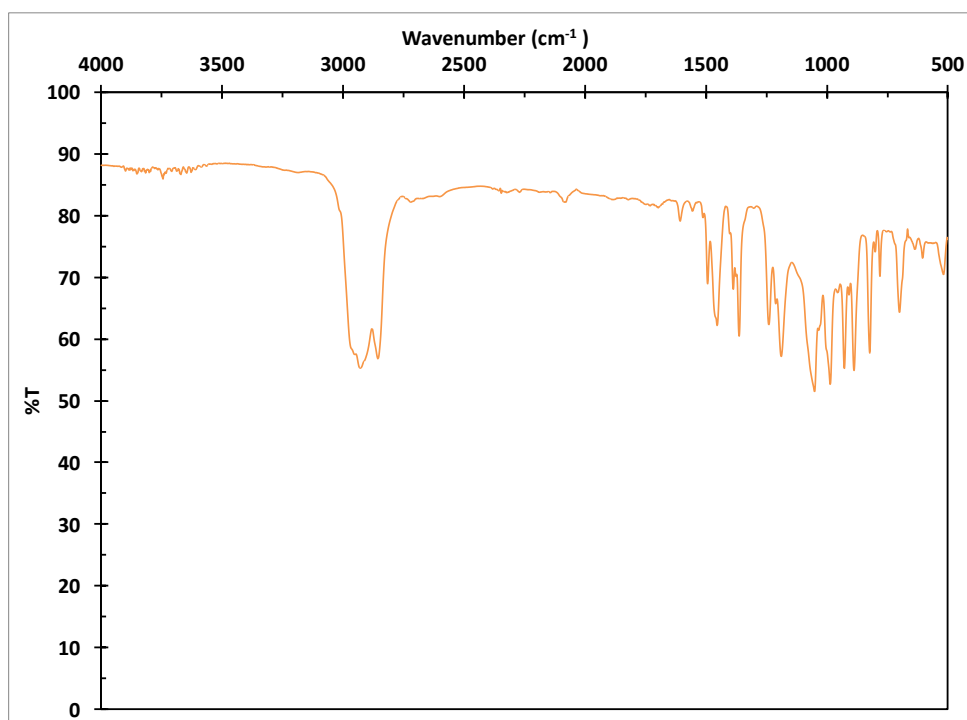


Figure S41: IR spectrum of isolated complex **1** in a Nujol suspension measured on KBr windows

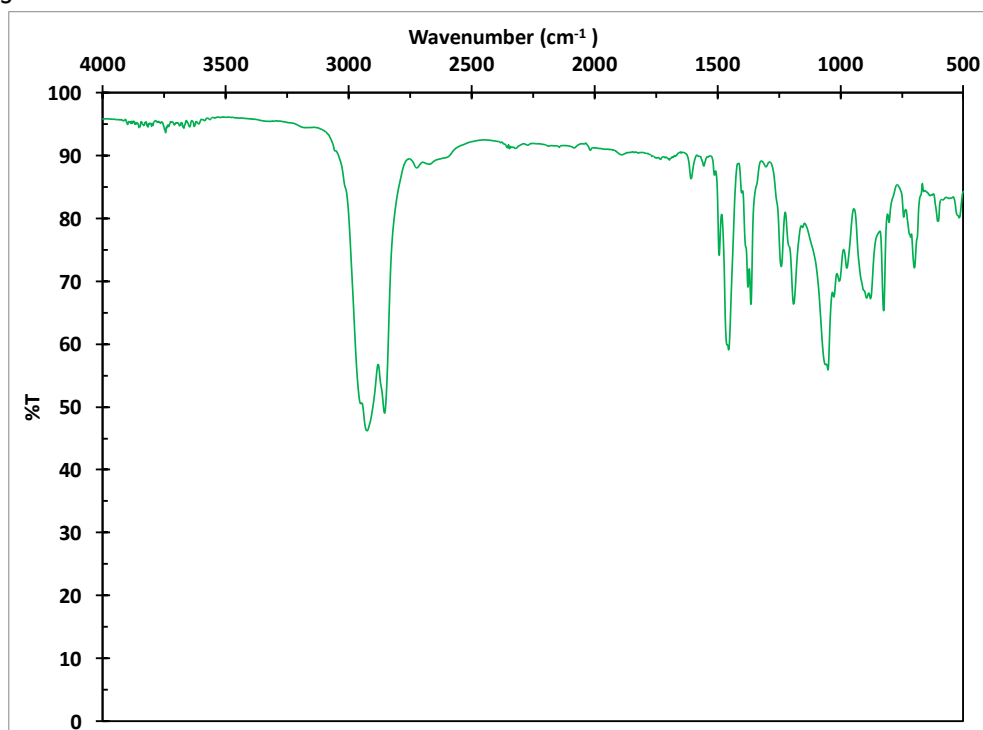


Figure S42: IR spectrum of isolated complex **2** in a Nujol suspension measured on KBr windows

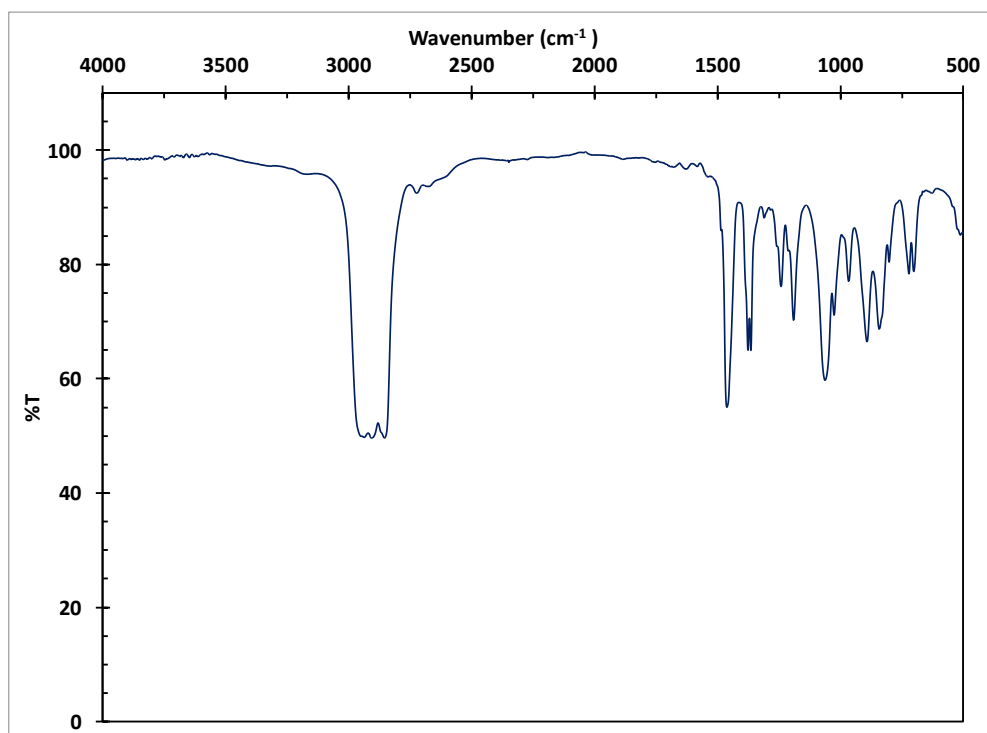


Figure S43: IR spectrum of isolated complex **4** in a Nujol suspension measured on KBr windows

GC-MS experiment

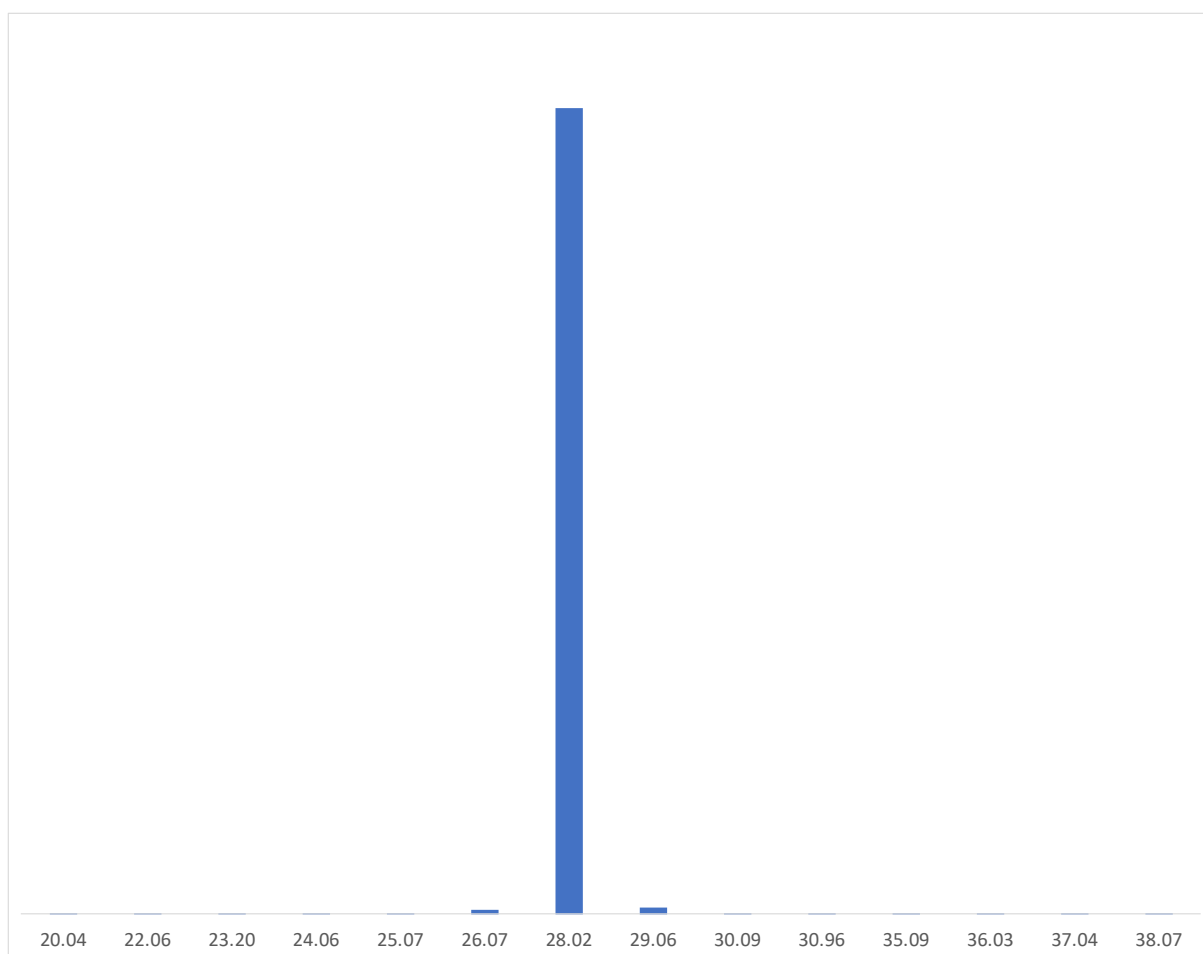


Figure S44: N₂ detection after full decomposition of complex **4** under Ar

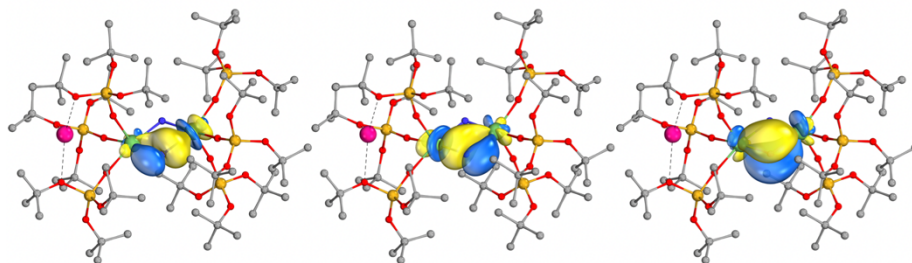
Computational Details

Density functional theory (DFT) calculations were performed with Turbomole 7.3.⁸ All open-shell calculations were spin unrestricted, using the hybrid functional PBE0.^{9,10} The cc-pVDZ basis set was used on all atoms, other than uranium on which cc-pVDZ-PP basis was used¹¹ (with the associated 60 relativistic effective core potential¹²). Grimme's D3 dampening function was used to account for dispersion interactions.¹³ Turbomole's m4 integration grid was used.

Quantum Theory of Atoms-in-Molecules (QTAIM) analyses were performed with AIMALL, with .wfx files generated by Molden2AIM.^{14,15} NBO 7.0 was used to obtain natural charges and Wiberg bond indices (WBI) in the natural atomic orbital basis.¹⁶ Molecular orbital visualisation, and intrinsic bonding orbital (IBO) analyses were performed with IBOView.¹⁷ Minimum quality bases for uranium and caesium were constructed from the cc-pVTZ-PP basis, in the same manner as previously described for other elements.¹⁷ Rudel et al. recently used IBO analysis on uranium by constructing Hartree-Fock orbitals from the def-TZVP basis (without polarisation functions) but obtained similar results to cc-pVTZ-PP.¹⁸ The uranium minimum quality basis included 7s, 6p, 6d and 5f valence orbitals. The four-exponent option was used for IBO analysis.

The presence of ITI was not probed computationally because (a) we did not optimise the heavy atom positions and (b) any possible ITI is small and present only for one of the U.

2 U(VI)/U(V):



4 U(VI)/U(VI):

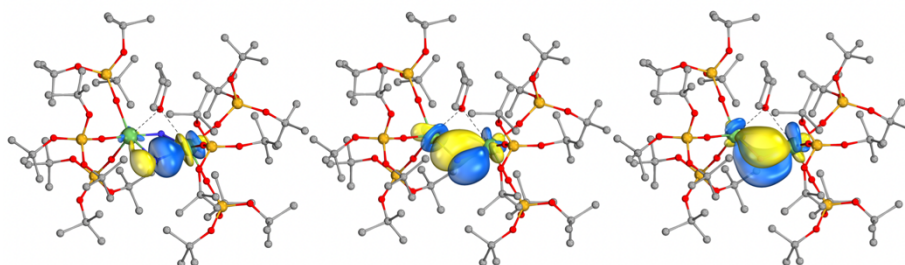


Figure S45: α spin IBOs of the U₂N₂ ring in **2** and **4**, on the opposite side of the ring to that shown in Figure 5 of the main text. Due to the C_i symmetry of **1**, orbitals of the opposite side of the ring are identical. The isosurfaces enclose 90% of the orbital.

References

1. L. Barluzzi, L. Chatelain, F. Fadaei-Tirani, I. Zivkovic and M. Mazzanti, *Chem. Sci.*, 2019, **10**, 3543 - 3555.
2. J. K. Peterson, M. R. MacDonald, J. W. Ziller and W. J. Evans, *Organometallics*, 2013, **32**, 2625-2631.
3. R. F. Jordan, C. S. Bajgur, W. E. Dasher and A. L. Rheingold, *Organometallics*, 1987, **6**, 1041-1051.
4. CrysAlisPRO, *Rigaku Oxford Diffraction*, release 1.171.41.96a 2021.
5. G. M. Sheldrick, *Acta Crystallogr., Sect. A*, 2015, **71**, 3-8.
6. G. M. Sheldrick, *Acta Crystallogr. C*, 2015, **71**, 3-8.
7. PLATON and A. L. Spek, *Acta Crystallogr. Sect. D*, 2009, **65**, 148-155.
8. F. Furche, R. Ahlrichs, C. Hättig, W. Klopper, M. Sierka and F. Weigend, *WIREs Comput Mol Sci* 2014, 4:91–100
9. J. P. Perdew, K. Burke, M. Ernzerhof, *Phys. Rev. Lett.*, 1996, **77**, 3865
10. J. P. Perdew, and M. Ernzerhof, *J. Chem. Phys*, 1996, **105**, 9982
11. K. A. Peterson, *J. Chem. Phys*, 2015, **142**, 074105
12. M. Dolg and X. Cao, *J. Phys. Chem. A*, 2009, **113**, 45, 12573–12581
13. S. Grimme, J. Antony, S. Ehrlich and H. Krieg, *J. Chem. Phys*, 2010, **132**, 154104
14. AIMAll (Version 19.10.12), Todd A. Keith, *TK Gristmill Software, Overland Park KS, USA*, 2019 (aim.tkgristmill.com)
15. W. Zou, D. Nori-Shargh, J. E. Boggs, *J. Phys. Chem. A* 2013, **117**, 1, 207–212
16. E. D. Glendening, C.R Landis, F. Weinhold, *J. Comput. Chem.*, 2019, **40**, 2234-2241
17. G. Knizia, *J. Chem. Theory Comput.* 2013, 9, 11, 4834–4843
18. S. S. Rudel, H. L. Deubner, M. Muller, A. J. Karttunen and F. Kraus, *Nat. Chem.*, 2020, **12**, 962-967